

**CAUDATE RESPONSES TO REWARD AND PUNISHMENT ARE PRESERVED IN  
HEALTHY OLDER ADULTS**

by

**Karin Cox**

B.A., Macalester College, 2003

Submitted to the Graduate Faculty of  
Arts and Sciences in partial fulfillment  
of the requirements for the degree of  
Master of Science

University of Pittsburgh

2007

UNIVERSITY OF PITTSBURGH  
SCHOOL OF ARTS & SCIENCES

This thesis was presented

by  
Karin Cox

It was defended on

April 18, 2007

and approved by

Howard Aizenstein, Assistant Professor, Department of Psychiatry

Mark Wheeler, Assistant Professor, Department of Psychology

Thesis Director: Julie Fiez, Professor, Departments of Psychology and Neuroscience

**CAUDATE RESPONSES TO REWARD AND PUNISHMENT ARE PRESERVED IN  
HEALTHY OLDER ADULTS**

Karin Cox, B.A.

University of Pittsburgh, 2007

An fMRI task developed in our laboratory has consistently identified the head of the caudate nucleus as a region with distinct responses to positive and negative outcomes (Delgado et al., 2000, Delgado et al., 2003, Tricomi et al., 2004). Subjects are engaged in a guessing game in which they receive monetary gain for correct guesses and monetary loss for incorrect guesses. Following a rewarding outcome, the caudate exhibits a relatively sustained hemodynamic response, while punishment responses are characterized by an early, high-amplitude peak response followed by a below-baseline dip in the caudate signal. This response pattern has been replicated across multiple studies in young adults; however, no published evidence has yet established the nature of reward and punishment signals in the striatum of healthy older adults. Therefore, the purpose of the current study was to establish a valid method for measuring reward- and punishment-related activity in healthy aging, and to describe any age-related effects on the hemodynamic responses found in the striatum. Twenty older adults (51-68 y) and thirteen young adults (18-28 y) were scanned as they completed the card-guessing task. Older adults exhibited robust, outcome-specific responses in the anterior caudate with bilateral foci of activation that overlapped with the activation found in the young adults. Furthermore, older adults retained key features of the typical caudate response profile, with a sustained increase in the signal following reward outcomes and a decrease in the signal following punishments. However, older adults did not demonstrate an early, high-amplitude peak in the punishment

response, which has been reported for earlier studies and was observed in the current young-adult sample. Finally, voxel-wise analyses identified two small clusters at or near the anterior caudate where older adults' signal appeared somewhat blunted relative to that of the young adults; similar blunting effects were found in a number of other regions throughout the brain. Overall, these findings validate the use of the card-guessing paradigm to assess outcome-specific responses in the striatum of older adults, and they point to some possible age-related effects that may be worthwhile to investigate in future studies.

## TABLE OF CONTENTS

<b>1.0</b>	<b>INTRODUCTION.....</b>	<b>1</b>
<b>1.1</b>	<b>METHODS.....</b>	<b>7</b>
<b>1.1.1</b>	<b>Participants.....</b>	<b>7</b>
<b>1.1.2</b>	<b>Behavioral tasks .....</b>	<b>8</b>
<b>1.1.3</b>	<b>fMRI data acquisition.....</b>	<b>10</b>
<b>1.1.4</b>	<b>Preprocessing of functional data .....</b>	<b>11</b>
<b>1.1.5</b>	<b>Statistical analysis of functional data.....</b>	<b>12</b>
<b>1.2</b>	<b>RESULTS .....</b>	<b>16</b>
<b>1.2.1</b>	<b>Behavioral results.....</b>	<b>16</b>
<b>1.2.2</b>	<b>Striatal activation patterns in older and young adults .....</b>	<b>17</b>
<b>1.2.3</b>	<b>Hemodynamic response of the caudate in older and young adults .....</b>	<b>21</b>
<b>1.2.4</b>	<b>Voxel-wise analyses of the group <math>\times</math> valence <math>\times</math> time and the group <math>\times</math> time interactions .....</b>	<b>23</b>
<b>1.3</b>	<b>DISCUSSION.....</b>	<b>28</b>
	<b>APPENDIX A .....</b>	<b>37</b>
	<b>APPENDIX B .....</b>	<b>54</b>
	<b>BIBLIOGRAPHY .....</b>	<b>64</b>

## **LIST OF TABLES**

Table 1. Functionally-defined clusters of interest sensitive to the valence x time interaction. ....	20
Table 2. Functionally-defined clusters of interest sensitive to the group x time interaction. ....	26

## LIST OF FIGURES

<b>Figure 1.</b> The original version of the card-guessing task.....	2
<b>Figure 2</b> The card-guessing task with modified timing parameters.....	9
<b>Figure 3.</b> Significant valence x time interaction effects in the bilateral caudate of older adult subjects.....	17
<b>Figure 4.</b> Overlap of older and young adults' activation maps for the valence x time interaction .....	18
<b>Figure 5.</b> Hemodynamic response functions extracted from activated clusters defined in the older and young adult groups separately. ....	21
<b>Figure 6.</b> Striatal clusters showing a significant group x time interaction.....	24
<b>Figure 7.</b> Hemodynamic response functions extracted from clusters sensitive to the group x time interaction.. ....	24
<b>Figure 8.</b> Clusters with significant group x time interaction effects .....	27
<b>Figure 9.</b> Two examples of hemodynamic timecourses from clusters outside of the striatum that showed a significant group x time interaction. ....	28
<b>Figure 10.</b> Consensus cluster of activation from five different studies using the guessing task, used to guide placement of manually-traced ROIs .....	41
<b>Figure 11.</b> Original and transformed structural images from the linear transformation procedure for the three oldest subjects in the sample. ....	43
<b>Figure 12.</b> Original and warped high-resolution structural images from the fully-deformable procedure for the three oldest subjects in the sample. ....	45
<b>Figure 13.</b> Illustration of a small distortion of the anterior caudate by the fully-deformable co-registration. ....	46

**Figure 14.** Average hemodynamic response functions extracted from original and co-registered functional datasets within a manually-traced bilateral region in the anterior caudate..... 48

**Figure 15.** Spatial extent of activation for the fully deformable and linear co-registration methods..... 50

**Figure 16.** Hemodynamic response function for a significant striatal cluster identified by the linear transform procedure..... 51

**Figure 17.** In the older adult group, putamen clusters demonstrating a significant main effect of time in response to the finger tapping task. .... 60

**Figure 18.** In the young adults, a right putamen cluster demonstrating a significant main effect of time in response to the finger tapping task..... 61

**Figure 19.** Hemodynamic responses extracted from the right putamen for the finger tapping task..... 62

## 1.0 INTRODUCTION

Activity patterns of the striatum are sensitive to a range of motivationally-salient events, including both reinforcing and noxious stimuli (Graybiel, 2005). Electrophysiological data from rodents and non-human primates have shown that appetitive and aversive stimuli modulate neuronal firing in all three of the striatal nuclei, including the putamen, the caudate nucleus, and the nucleus accumbens (Ravel, Legallet, & Apicella, 2003; Roitman, Wheeler, & Carelli, 2005; Schultz, Tremblay, & Hollerman, 2000; Williams & Eskandar, 2006). These findings in animal subjects are consistent with functional MRI studies in humans, which have demonstrated robust striatal responses to a diverse array of positive and negative events, including monetary gains and losses (Delgado, Nystrom, Fissell, Noll, & Fiez, 2000), juice reinforcers (O'Doherty et al., 2004), and pain-predictive cues (Seymour et al., 2004).

While responses to reward- and punishment-related events can be observed across the anatomical divisions of the striatum, the degree to which the various subregions are engaged by these stimuli is thought to depend on the specific task context. In humans, the caudate nucleus has been suggested to be a region that is selectively responsive to outcomes that are perceived to be contingent upon one's own actions (Tricomi et al., 2004, O'Doherty et al., 2004). A card-guessing task developed in our lab (Delgado et al., 2000) is an example of this kind of scenario.

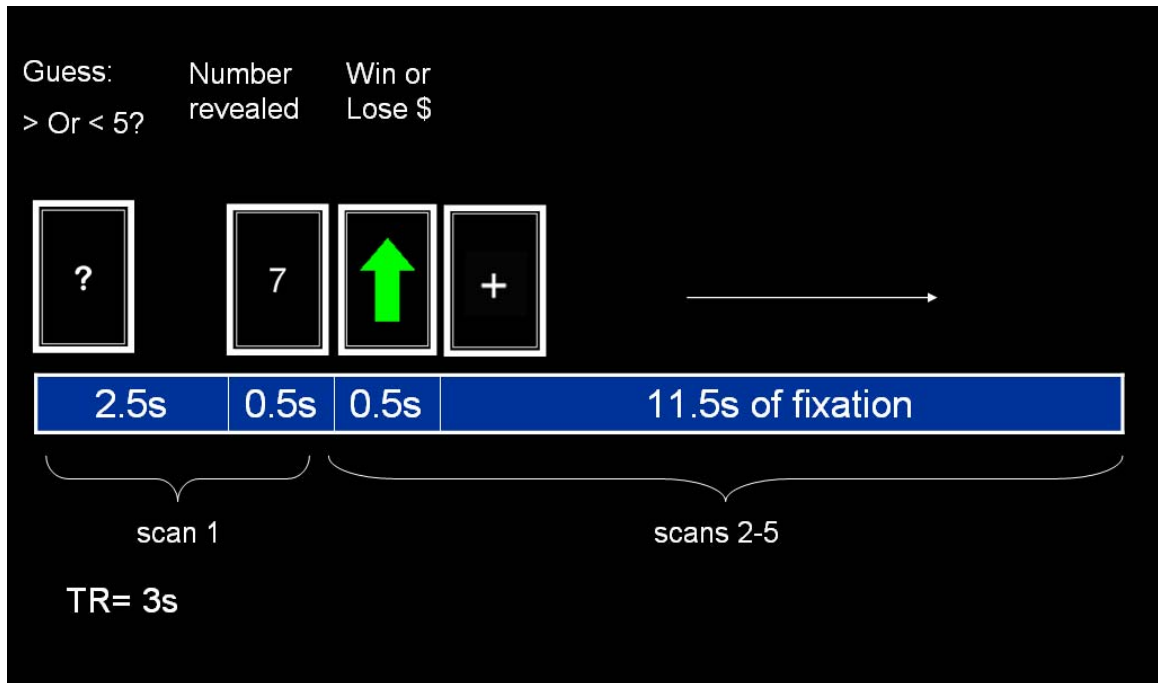


**Figure 1.** The original version of the card-guessing task (also known as the “gambling task”, Delgado et al., 2000). The figure shows an example of a predetermined “reward” trial.

On each trial of this task, subjects are instructed to guess the value of a concealed playing card (Figure 1). Following each guess, the subject is shown either a green arrow, indicating a correct guess and a small monetary reward, or a red arrow, indicating an incorrect guess and a small monetary loss. Across a number of replications (Delgado, Locke, Stenger, & Fiez, 2003; Tricomi, Delgado, & Fiez, 2004; Tricomi, Delgado, McCandliss, McClelland, & Fiez, 2006), the guessing task has consistently revealed hemodynamic responses in the caudate that discriminate between these rewarding and punishing outcomes. Specifically, a reward outcome tends to evoke a gradual signal increase followed by a relatively slow return to baseline, while a punishment outcome results in a rapid, high-amplitude peak followed by a decrease in the signal below baseline levels.

The card-guessing task (Delgado et al., 2000) is one of several fMRI paradigms that show robust activation of the caudate (as well as other regions of the basal ganglia) when subjects

perform simple tasks in order to earn rewards or avoid punishments (e.g., Knutson, Adams, Fong, & Hommer, 2001; Nieuwenhuis et al., 2005). A growing area of speculation concerns how the striatal activity evoked by these incentive-driven tasks might be modulated in populations that may process rewards and punishments differently than healthy young subjects do. Since neuroimaging paradigms that generate striatal activity are often assumed reflect an underlying influence of the dopamine system (Knutson & Gibbs, 2007), several researchers have begun to use these tasks to study psychiatric or neurological conditions in which dopaminergic dysfunction is thought to play an important role, including Parkinson Disease (e.g., Cools, Lewis, Clark, Barker, & Robbins, 2007; Kunig et al., 2000). However, an important but often underappreciated challenge in studying patients with Parkinson Disease (PD) is their advanced age. Behavioral studies of reward-related processing in PD (Cools et al., 2006; Frank et al., 2004; Swainson et al., 2000) often report data from “old-onset” PD patients in the mild-to-moderate stages of the disease, with a typical patient sample ranging from 50 to 75 years of age. Because imaging experiments in PD are likely to involve a similar age range, future studies of how rewards and punishments modulate the BOLD signal in a patient population would benefit from a baseline measurement of similar phenomena in healthy older adults.

Surprisingly, no published fMRI reports have specifically focused on reward- and punishment-related responses in normal aging (although some preliminary data have been described, see Larkin et al., 2006 and Marshner et al., 2005). A demonstration that rewards and punishments reliably modulate striatal activity in an older adult population could open up a number of new areas of future research in this age group, both in patients and in healthy individuals. Questions regarding the neural underpinnings of outcome-related processing in healthy older adults have attracted increased interest recently in part due to age-related

anatomical changes that may affect older adults' reward circuitry (see Marschner et al., 2005, for a review). Even healthy aging has been associated with a gradual loss of dopamine neurons in the substantia nigra (Cabello, Thune, Pakkenberg, & Pakkenberg, 2002), and correlations between age and striatal volume loss have been consistently observed (e.g., Raz, Torres, & Acker, 1995). In addition to these neuroanatomical differences, older adults have also exhibited altered patterns of behavioral responses to positive and negative outcomes. Age-related impairments have been found in the context of probabilistic reversal learning, with older adults requiring a greater number of trials to learn new stimulus-reward associations (Mell et al., 2005), and a subset of older adult subjects have demonstrated suboptimal decision-making behavior in the Iowa Gambling Task (Denburg, Recknor, Bechara, & Tranel, 2006). Therefore, the establishment of some kind of method to assess older adults' hemodynamic responses to motivationally-important outcomes could be useful for future investigations designed to relate neural activity to any of these age-related behavioral or anatomical differences. However, before these more extensive neuroimaging studies can be conducted (and before similar studies can be conducted in patient populations), it is important to address several methodological issues specific to an older adult population.

The physiological and anatomical changes that accompany healthy aging present a number of concerns that may have important implications for experimental design and analysis. First, it is common for older adults' fMRI data to be 'noisier' than young adult data (Huettel, Singerman, & McCarthy, 2001), such that statistically reliable effects can be difficult to establish. Second, event-related fMRI experiments using passive sensory stimulation (Richter & Richter, 2003) and simple motor execution (Aizenstein et al., 2004) have shown that the hemodynamic signal in older adults may exhibit a relatively slow decay to baseline, such that

older subjects' time courses appear prolonged in comparison to those of younger subjects. The observation of this signal difference in basic sensorimotor tasks suggests that the sustained response might be due to a fundamentally physiological cause (e.g., changes in vascular structure, D'Esposito, Deouell, & Gazzaley, 2003) that could influence any imaging experiment done in an older population. Finally, the gradual atrophy of both cortical (Raz et al., 2004) and subcortical regions (Raz, Torres, & Acker, 1995) has been well documented in healthy older adults; the resulting anatomical variability raises questions of how to best align subjects' functional datasets when group-level analyses are performed.

In light of these concerns, we designed a study to establish a valid means for measuring older adults' reward- and punishment-related responses within the context of our card-guessing task (Delgado et al., 2000). The purpose of this preliminary experiment was to provide baseline data that will inform future investigations in both healthy and impaired older-adult populations; all of the above-mentioned methodological concerns were addressed. First, we addressed the problem of increased variability in older adults by scanning a greater number of subjects ( $n = 20$  older adults) than we have typically reported in previous investigations using the guessing task (c.f. Delgado et al., 2000). Second, we modified the slow event-related design of the guessing task to account for the possibility of hyper-extended hemodynamic response functions in older adults; in particular, we increased the inter-trial fixation interval by several seconds. Finally, we employed a novel fully-deformable co-registration procedure as a strategy for warping the functional datasets into a common space.

A secondary goal of this study was to describe the time course of the striatal signal that is observed when older adults complete the guessing task, and to identify how its response function may differ from that observed in younger subjects. Therefore, we also scanned a group of

healthy young adult subjects using the same protocol that we had designed for use with the older adults. This allowed for a general assessment of any age-related differences that might be observed in the striatal response profile. Awareness of any young- versus old-adult differences in the hemodynamic response function would be informative at a methodological level; for example, age effects on the function's shape may imply that some task designs and analysis methods (e.g., the use of certain response assumptions when modeling rapid event-related data) may not be appropriate to use in older subjects. It is important to note that our goals in making this young vs. old comparison were largely descriptive; this experiment was not designed to test any specific predictions of how aging may affect the way that the brain processes reward and punishment. Future experiments could be designed to disentangle how the anatomical and behavioral changes observed across the lifespan might be related to any age-related differences observed in the card-guessing task.

In summary, the primary aim of the present study was to establish a valid means of measuring reward- and punishment-related hemodynamic responses in the striatum of older adults. Using modified temporal parameters for the card-guessing task and a high-dimensional co-registration procedure, we were able to demonstrate that reliable caudate responses can be found in healthy older adults, and we compared the features of the resulting hemodynamic responses to those of healthy younger subjects.

## 1.1 METHODS

### 1.1.1 Participants

Healthy right-handed “older” adults (defined as 50-70 years of age) and younger adults (18-35 years) were recruited with flyers posted around the University of Pittsburgh campus and in the surrounding community, as well as advertisements placed in newsletters targeted towards a senior audience. The age range defined for the older adult group was consistent with the typical demographics reported in studies of patients with mild-to-moderate Parkinson’s Disease (e.g., Swainson et al., 2000). Potential subjects were excluded from participation if they had any history of illicit drug use, stroke, or a major neurological or psychiatric disorder. Participants were required to be “generally healthy” (no current serious medical condition that required regular attention from a physician) and were not enrolled in the study if they were currently taking any psychotropic medications. Participants who satisfied these inclusion and exclusion criteria were further screened for depression and general cognitive impairment; subjects were included if they scored  $\leq 13$  on the Beck Depression Inventory (BDI-II) and  $\geq 26$  on the Mini-Mental State Examination (MMSE, Folstein, Robins, & Helzer, 1983), respectively.

Twenty-nine older adults and twenty-one young adults passed the eligibility criteria and were enrolled in the study. Three older adults did not complete the imaging protocol for reasons of either claustrophobia, in the case of one subject, or general discomfort in the scanner, in the case of two subjects. Two young subjects also failed to complete the protocol due to technical difficulties and claustrophobia, respectively. No data from these participants were included in analyses. Of the subjects who completed the entire experiment, data from three young adult subjects and three older adult subjects were removed due to excessive head motion, and data

from two young adults and a single older adult were removed due to observations of subjects' drowsiness during the scanning session. Data from one additional older adult were removed based on the finding of a scanner-related artifact in that subject's functional data. Two older subjects and one young subject contributed only a subset of the total number of runs for the primary behavioral task (fewer than the 8 total runs of the card-guessing task), with one older adult and one young adult contributing 7 runs, and one older adult contributing 6 runs. Loss of the single run in the young adult was due to a technical problem. One of the older adults ended the session early due to "restlessness" in the scanner, while the other older adult's session was terminated due to back discomfort. Data from these subjects were included in analysis. The final dataset reported for all analyses of the card-guessing task included 20 older adult participants (range 51-68y, mean $\pm$ -SD = 57.60 $\pm$  4.63) and 13 young adult participants (range 18-28y, mean $\pm$ -SD = 22.31 $\pm$ -3.276).

### **1.1.2 Behavioral tasks**

During the scanning session, subjects completed 8 runs of the card-guessing task, with 12 trials per run. The task was programmed using E-Prime software (Psychology Software Tools, Pittsburgh, PA) and presented in the scanner environment using the Integrated Functional Imaging System (IFIS-SA, Invivo, Gainesville, FL). Subjects made their responses to the guessing task with the index- and middle-finger buttons of a response glove on their right hand. Response and reaction time data were recorded for each trial.

As in our previous work with the guessing task (Delgado et al., 2000), the temporal structure of the task was based on a slow event-related design. A trial began with the presentation of a concealed playing card for 2.5s (Figure 2).

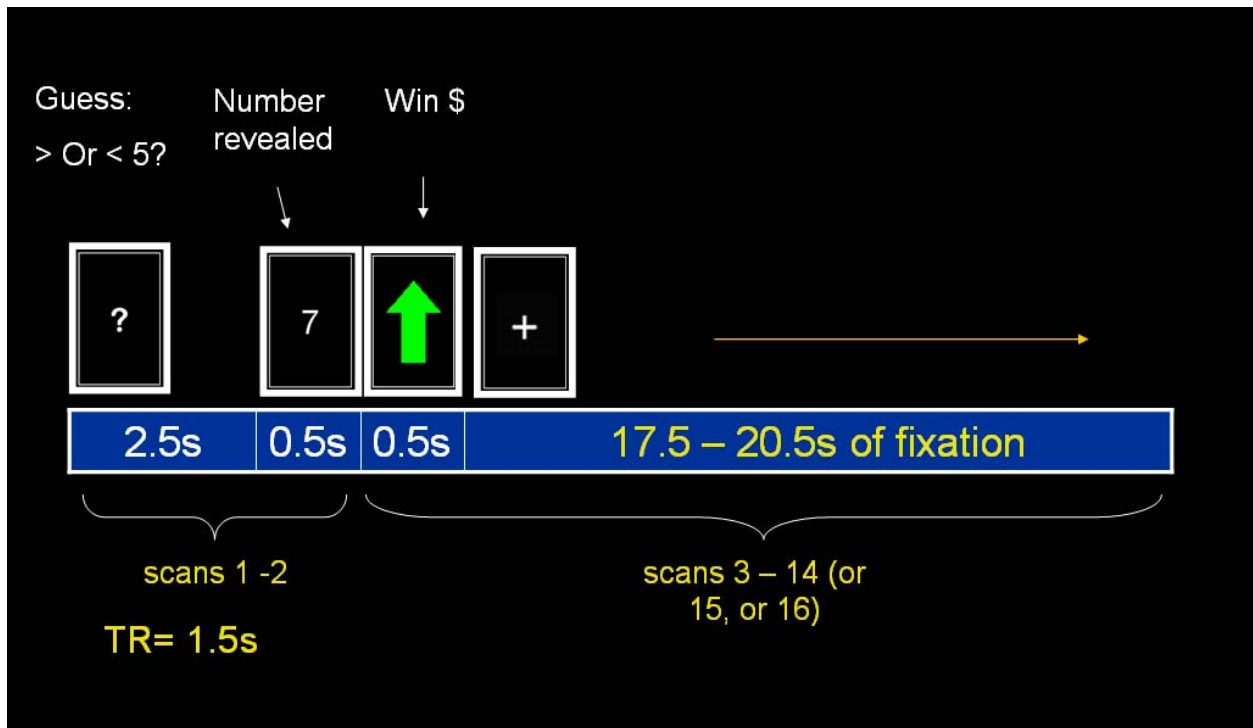


**Figure 2** The card-guessing task, with the modified timing parameters that were used for the present study.

While the card was present on the screen, subjects used a button press to indicate their guess of whether the value of the card was greater or less than 5. Following this choice period, the number was revealed for 0.5 s, followed by a 0.5 s outcome display with either an upwards-pointing green arrow to indicate a correct guess, or a downwards-pointing red arrow to indicate an incorrect guess. The trial ended with a long inter-trial fixation period of at least 17.5 s to accommodate the possibility that older subjects' hemodynamic responses would be slow to return to baseline levels. Basic perceptual studies of the BOLD signal in older adults suggest that this interval should be sufficient for responses to return to baseline (Richter & Richter, 2003); however, given the lack of pre-existing data on reward-related processing in older adults, an additional duration of jitter (1.5-3ms) was added to a random subset of trials so that a deconvolution method could be used to estimate responses in the event that they persisted beyond the boundaries of a single trial.

All participants read written instructions for the card-guessing task and received 12 trials of practice with the task before entering the scanner. Participants were told that for each correct guess, they would earn \$4.00, and for each incorrect guess, they would lose \$2.00. In reality, the same fixed sequence of outcomes was predetermined for every subject, such that half of their guesses would be correct and half would be incorrect. At the end of the session subjects were debriefed regarding the nature of the task and paid \$90 for their participation.

As part of the same experimental session, both participant groups also completed a bimanual finger tapping task; the procedure, analyses, and results for this task are described in Appendix B. The order of the card-guessing and finger-tapping tasks was counterbalanced across participants. The finger tapping task was administered in order to support future analyses that may address the question of whether any observed age effects in the striatum are general to all tasks or specific to reward-processing per se.

### **1.1.3 fMRI data acquisition**

All subjects were scanned at the UPMC Presbyterian Hospital MR Center with a 1.5T GE Signa whole-body scanner. Each 1hr 15 min scanning session began with the acquisition of structural data. For purposes of inter-subject registration, we collected high-resolution whole-brain structural data (SPGRs) as well as lower-resolution axial images. Low-resolution data were acquired in 40 contiguous oblique slices parallel to the AC-PC line, with an inplane resolution of  $.9375 \text{ mm}^2$  and a voxel depth of 3.8 mm. Functional data were collected in 20 oblique slices (resolution  $3.75 \times 3.75 \times 3.8 \text{ mm}$ ) using a one-shot forward spiral pulse sequence ( $\text{TR} = 1500$ ,  $\text{TE} = 35\text{ms}$ ,  $\text{FOV} = 24\text{cm}$ ,  $\text{flip angle} = 70^\circ$ ). Altogether, there were 8 runs of functional acquisition, with each run lasting 4 min and 37.5 s. Functional slices overlapped with a subset

of the low-resolution structural slices and included 15 slices superior and 5 slices inferior to the AC-PC line. This slice prescription allowed for complete coverage of the dorsal and ventral striatum in all subjects, as well as a large portion of cortex and the most superior regions of the cerebellum. Functional coverage did not include some dorsal regions of frontal and parietal cortex, as well as some ventral regions of frontal and temporal cortex (as well as the majority of the brainstem and the cerebellum).

#### **1.1.4 Preprocessing of functional data**

The raw data were preprocessed using the NeuroImaging Software package (NIS-3.6, developed at the University of Pittsburgh and Princeton University), and Automated Image Registration (AIR 3.08, Woods, Cherry, & Mazziotta, 1992). Functional images were corrected for subject movement; runs in which motion exceeded 4 mm or 4° were excluded from subsequent analysis. (This step resulted in the removal of the final run from each of two older subjects' datasets). For each voxel of the motion-corrected images, a baseline correction was applied to correct for signal differences between runs, and a linear detrending step was used to adjust for gradual signal drift within runs.

In preparation for group-level statistical analyses, we used the older adults' preprocessed data to compare alternative methods for the spatial normalization of the structural and functional volumes. The results of this comparison are reported in Appendix A. The method used in the present experiment was selected on the basis of this preliminary comparison.

To spatially normalize both older and young adults' brains, we used a fully-deformable co-registration procedure (Wu, Carmichael, Lopez-Garcia, Carter, & Aizenstein, 2006; Wu, Mazurkewicz, Nable, & Aizenstein, 2006) to warp the high-resolution SPGR images from each

subject to a local reference brain. In one previous report (Wu et al., 2006), a comparison between the fully-deformable procedure and two other nonlinear warping programs (from the AIR package (Woods, Grafton, Watson, Sicotte, & Mazziota, 1998) and the SPM package (Friston et al., 1995)) provided preliminary evidence that the fully-deformable approach results in superior co-registration. The algorithm on which this method is based is available through the free public library of the Insight Segmentation and Registration Toolkit (ITK, <http://www.itk.org>) A more detailed description of the fully-deformable registration procedure is included in Appendix A. The reference brain used in the current study was the high-resolution SPGR image collected from a 29-year-old male subject who had not contributed to the current functional dataset.

The deformation defined for each subject's structural data was subsequently applied to all functional volumes for that individual. Following spatial normalization, intensity values of each functional volume were normalized with a multiplicative correction that set the global mean intensity at an arbitrarily-determined value of 2000. Intensity normalization was followed by a spatial smoothing step (3D Gaussian filter, 4 mm FWHM) to attenuate the effects of anatomical variability between subjects.

### **1.1.5 Statistical analysis of functional data**

The timing parameters used for the card-guessing task allowed for two potentially valid means of estimating the hemodynamic timecourses evoked by the reward and punishment trials. Under the assumption that the response returns to baseline within the minimum 17.5s fixation interval, timecourses for each subject can be determined by simple averaging: Timepoints from the first 21s of each trial (or with a TR of 1.5s, the first 14 scans) are averaged for each condition

in order to determine the mean hemodynamic response; data from the extra timepoints (i.e., the additional scans that constituted the jitter) are discarded in this analysis. However, if hemodynamic responses do not return to baseline within the minimum 17.5s fixation interval, the simple averaging approach is rendered invalid, since this observation implies that responses to the individual trials overlapped in time. In this case, the shape of the hemodynamic responses for each condition can be estimated by submitting the entire jittered dataset to a GLM-based deconvolution algorithm that does not assume a standard response function (e.g., AFNI 3dDeconvolve, Cox, 1996). Based on observations that hemodynamic responses in the striatum did appear to resolve to baseline within a 17.5s fixation period, the timecourse estimates presented for the current experiment are based on the simple-averaging approach. Therefore, for each voxel and each subject, average intensity values were computed for the first 14 timepoints of the reward and punishment conditions. These subject-level averages were then submitted to group-level statistical analyses.

Analysis of the functional timecourse data consisted of two stages. For the initial set of analyses, data from the older- and young-adult subjects were divided into two separate datasets, so that voxel-wise definition of clusters of interest could be determined independently for the two age groups. This separate groups approach was chosen based on the following advantages. First, analyses that are restricted within the age groups can address the question of whether or not older adults' responses would be sufficiently reliable to allow for definition of clusters that meet a rigorous statistical threshold. Second, the independent groups analysis allows for comparison of age-related effects on both the spatial focus and extent of any observed striatal activation. Finally, the independently-defined striatal clusters can be used to extract functional timecourses that are based on the most reliably activated voxels for each age group. If the clusters sensitive

to the valence x time interaction were defined with a combined dataset of both young and old subjects, then it is possible that region definition would be biased by the younger group's data, especially if functional effects in this group are more powerful. Timecourses extracted from clusters that are biased in this way might create a misleading estimate of the older adults' responses to the task (c.f. Aizenstein et al., 2004).

For the separate-groups analysis, functional data were submitted to a 2-way repeated measures voxel-wise ANOVA, with valence (reward vs. punishment) and time (an index of the 14 scans in each trial, T1-T14) as factors. In order to reduce the likelihood that edge voxels or voxels from regions of high susceptibility would be included in the analysis, all voxelwise analyses were masked with the thresholded functional image from a single older adult subject. Primary analyses were performed with an *a priori* focus on the dorsal and ventral striatum, including the caudate nucleus, the putamen, and the nucleus accumbens. Activated voxels were identified as those that demonstrated a significant valence x time interaction at  $p < 0.0001$ . In order to protect against Type-I errors, a contiguity threshold was applied to each activation map in order to define reliably activated regions of interest (Forman et al., 1995). Minimum cluster sizes were determined using the AFNI AlphaSim program (Cox, 1996) such that a significant cluster was associated with a corrected  $p$  value of  $< 0.05$ . For all statistical tests reported for the present experiment, this cluster threshold was determined to be three contiguous voxels. Following the identification of activated clusters, statistical maps were converted into the standard atlas space of Talairach and Tournoux (Talairach & Tournoux, 1998) in order to determine the anatomical focus of each cluster of interest.

The statistical maps generated by the separate-groups analysis were then used to qualitatively compare the general distribution of striatal activation in the older versus the young

adult groups, as well as to statistically compare the shape of each group's hemodynamic responses to reward and punishment trials. For anatomical regions that were associated with significant and overlapping clusters in both age groups (e.g., the right or left head of the caudate nucleus), old and young adults' hemodynamic responses were compared by extracting average timecourse data from each group's cluster. To reduce variance associated with arbitrary baseline differences, timecourses from each cluster for each subject were normalized with a multiplicative correction such that the mean of all timepoints for all conditions was set to 2000. These normalized timecourses were submitted to two kinds of analyses. First, differences between the timecourses were assessed using a 3-way mixed ANOVA, with age group as a between-subjects factor and valence and time as within-subjects factors; effects of interest were the 3-way group  $\times$  valence  $\times$  time interaction and the 2-way group  $\times$  time interaction. A significance threshold of  $p < 0.05$  was applied to these interaction effects. Second, for each group and each cluster, the reward and punishment responses were compared using two-tailed  $t$ -tests at three timepoints (T4, comprising the period 1.5-3s following onset of the outcome display, and T7 and T8, comprising the period 6-9s following onset of the outcome display). The purpose of these contrasts was to assess whether or not the response profiles in the current study retained similar properties as have been noted in earlier reports of the card-guessing task. The T4 timepoint was tested in order to determine if the early punishment response was associated with a higher amplitude than was found for the reward response at that timepoint; the choice of this timepoint was based on previous studies showing an early "punishment peak" during this time period (e.g., Delgado et al., 2003). The T7 and T8 timepoints were chosen based on previous studies that have shown that the reward response is of higher amplitude than the punishment response during this period (Delgado et al., 2003; Tricomi et al., 2006),

suggesting a more sustained response to rewards than to punishments. All *t*-test results were interpreted with a significance threshold of  $p < 0.05$ .

For the second stage of analysis, older and young adult data were combined so that voxelwise analyses could be performed on a composite dataset. The advantage of this approach relative to the separate-groups analysis is its sensitivity to group-level effects that are not constrained to spatially coincide with the clusters that are defined in each group separately. To test for group-level differences at the voxelwise level, the full set of functional data were submitted to a similar 3-way group  $\times$  valence  $\times$  time ANOVA as was used in the analysis of the separated dataset. This analysis was used to produce two statistical maps: an activation map for the 3-way group  $\times$  valence  $\times$  time interaction, and an activation map for the 2-way group  $\times$  time interaction. Significant clusters of interest were identified using a threshold of  $p < 0.0001$ ; contiguity thresholds were set using the same procedure as described for the separate-groups analysis.

## 1.2 RESULTS

### 1.2.1 Behavioral results

Older and young adults' reaction times did not significantly differ for the card-guessing task (mean $\pm$  SE = 712.82 $\pm$ 60.67 ms for old, 663.99 $\pm$ 36.46 ms for young;  $t(31) = -.734$ ). A coarse-level analysis of the two groups' response patterns showed no significant differences in the rates at which each response option was chosen, with both older and young adult subjects

choosing the “greater than 5” option approximately half of the time (56% choice of “> than 5” in the older adult group, and 51% choice of this option in the young adult group).

### 1.2.2 Striatal activation patterns in older and young adults

For the first stage of analysis, voxelwise effects were assessed in the two age groups independently. Voxelwise analysis of the older-adult dataset identified a significant valence x time interaction in the head of the caudate nucleus. Activated clusters were located bilaterally with peaks in both the left caudate [-13,11,8] and the right caudate [13,15,4]. The spatial extent of this striatal activation is shown in Figure 3. The left and right clusters included a total of 11 and 10 active voxels, respectively.

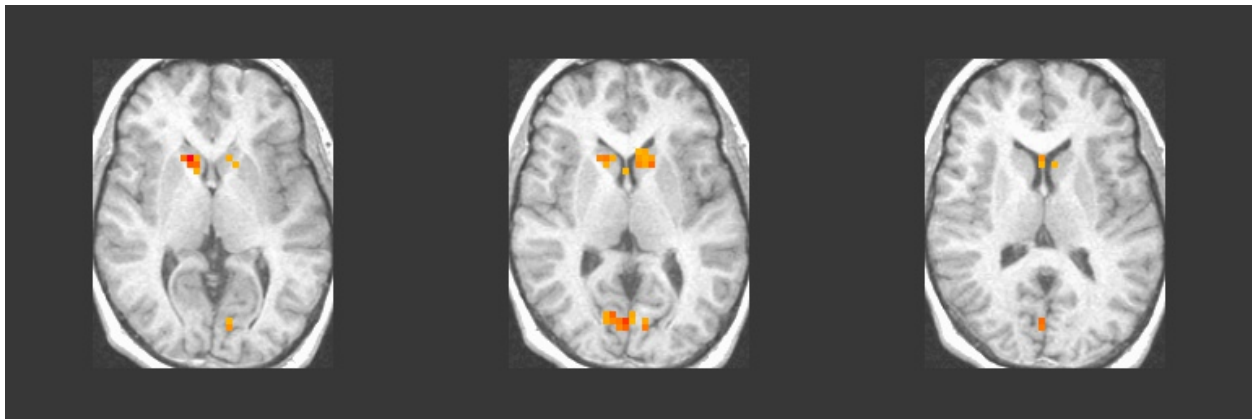


**Figure 3.** Significant valence x time interaction effects in the bilateral caudate of older adult subjects. Results are thresholded at  $p < 0.0001$  with a contiguity threshold of 3 significant voxels. Images are shown according to radiological convention (right = left).

A similar focus of caudate activation was found for the valence x time effect in healthy young subjects, with cluster peaks located at [-8,18,4] for the left caudate and [15,18,4] for the right caudate. In order to identify any common voxels between the older and young adults?

activated clusters, the statistical maps for the two groups were overlaid. The resulting overlap map is shown in Figure 4.

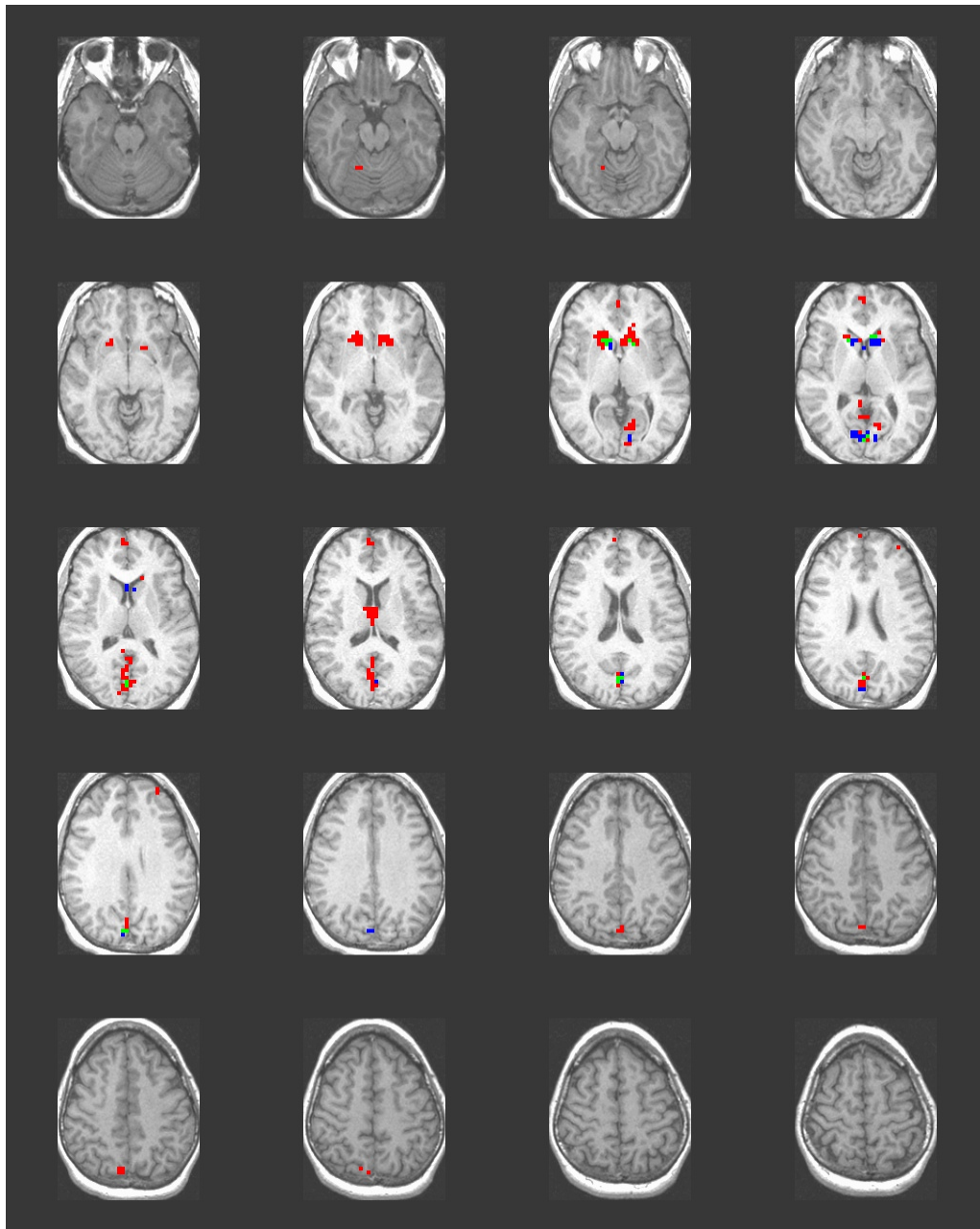


**Figure 4.** Overlap of older and young adults' activation maps for the valence x time interaction;  $p < 0.0001$  in each group. Red voxels = Active in young subjects only, blue voxels = Active in old subjects only, green = Active in both young and old subjects.

Overlap of the two age groups' activation maps revealed common voxels in both caudate nuclei, with an overlap region of four voxels on the left and five voxels on the right. Within the

striatum, all overlapping voxels were restricted to the anterior caudate (and the nearby white matter) on the two slices immediately superior to the slice containing the anterior and posterior commissure. Older adults had only a few active voxels that lay outside of this dorsal – ventral extent; in contrast, younger adults showed a more extensive pattern of striatal activation, with active clusters spreading to more ventral regions, including bilateral regions in the ventral putamen.

Beyond our *a priori* focus on the striatal nuclei, a few clusters sensitive to the valence  $\times$  time interaction were found in posterior regions of cortex (in both the old and young group) as well as in the frontal cortex, thalamus, and right cerebellum (for the young subjects only). All active regions for the young and old groups are listed in Table 1.

**Table 1.** Functionally-defined clusters of interest sensitive to the valence x time interaction,  $p < 0.0001$ , contiguity threshold = 3 voxels. Clusters were defined independently for the old and young adults. TT coord. = coordinates in Talairach atlas.

Location	Older adults			Young adults		
	Peak <i>F</i> value	PeakTT coord.	Cluster size	Peak <i>F</i> value	PeakTT coord.	Cluster size
Left caudate	4.17	[-13,11,8]	11	5.77	[-8,18,4]	34
Right caudate	5.15	[13,15,4]	10	7.48	[15,18,4]	32
Within 5mm of caudate (septum)	3.76	[1,14,12]	3			
Right posterior cingulate				4.36	[4,-45,12]	3
Right medial frontal gyrus/BA 10				6.42	[5,55,12]	13
Left superior frontal gyrus				4.13	[-29,55,27]	3
Right precuneus/Right BA 7				5.63	[5,-75,42]	11
Right cuneus	4.67	[2,-76,8]	19	6.13	[1,-80,12]	56
(two separate foci in older adults)	4.91	[6,83,27]	7			
Left cuneus	4.06	[-9,-79,8]	4			
Left lingual gyrus				4.78	[-14,-64,4]	9
Right thalamus				5.96	[1,-10,15]	12
Right cerebellum				3.98	[16,-53,-16]	3

### 1.2.3 Hemodynamic response of the caudate in older and young adults

Older adults demonstrated the expected pattern of caudate activation to reward and punishment outcomes, with a reward response that was sustained relative to the response observed for punishment. Figure 5 shows the timecourse data from the left and right caudate clusters that showed a significant valence  $\times$  time effect in the older adult group.

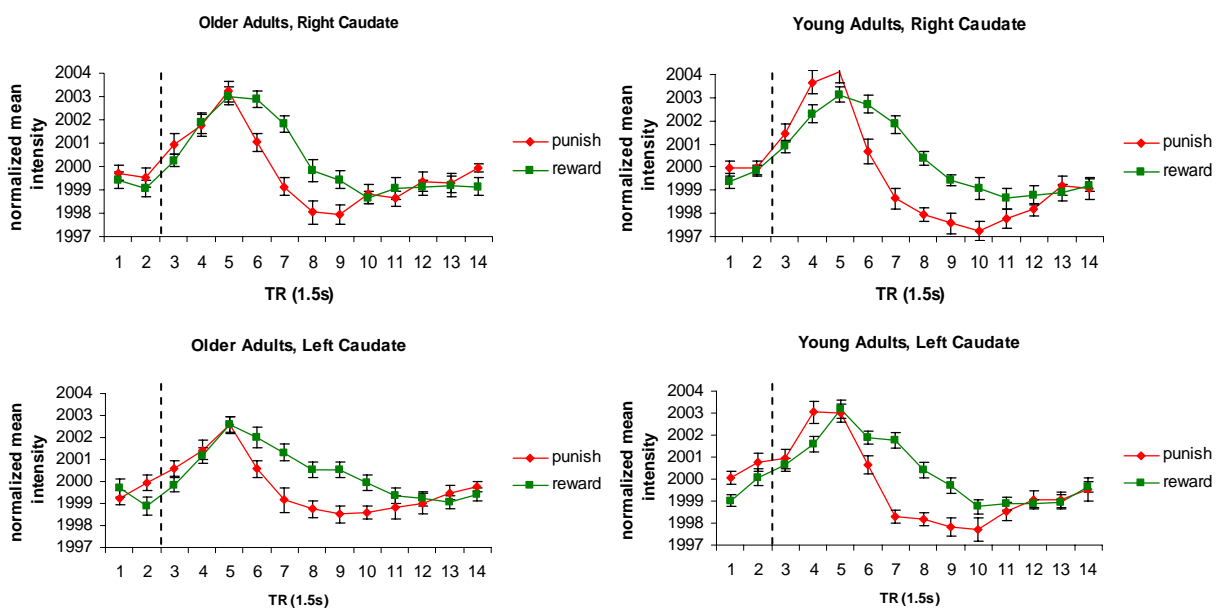


**Figure 5.** Hemodynamic response functions extracted from activated clusters defined in the older and young adult groups separately. Dashed line indicates onset of the outcome display. Error bars show standard error of the mean.

T-tests performed at timepoint T4, which constituted the period 1.5-3.0 s following the onset of the outcome display, failed to find evidence of an early punishment peak in older adults: The amplitude of the punishment response was not significantly greater than the amplitude of the reward response at that timepoint (for the left,  $p = .569$ ; for the right,  $p = .841$ ). In contrast, the young adult group did show evidence of a greater punishment signal during this time period (for the left,  $p = .005$ ; for the right,  $p = .003$ ).

One possible explanation for the lack of the early punishment peak in the older adults might be related to the fact that the clusters defined in this group extended into a more dorsal portion of the striatum than the young adults' clusters did. If the underlying neural generator of the early punishment peak was restricted to a ventral region of the caudate, then the presence of these relatively dorsal voxels in the older adults' cluster might obscure this feature of the punishment response. Therefore, as a follow-up analysis, older adults' timecourses were examined for the two small and relatively ventral clusters that had been identified as region of direct overlap between the two age groups. Responses isolated to these smaller clusters were similar to those found for the older adults' functionally-defined clusters, with no apparent difference between the punishment and reward peaks.

T-tests performed at timepoints T7 and T8, which comprised the period 6-9s following the onset of the outcome display, confirmed that older adults' responses to reward and punishment did significantly differ at these two timepoints ( $p$  values  $< 0.005$  for both timepoints and in both the left and right nuclei). Young adults also showed reliable divergence of the reward and punishment responses at these timepoints ( $p$  values  $< 0.0005$  for both timepoints and both nuclei).

In order to test for differences between older and young adults' response profiles, timecourses were compared for the left and right caudate separately. The 3-way group  $\times$  valence  $\times$  time interaction failed to reach significance for either the left caudate ( $F(13,403) = 1.269, p = .229$ ) or the right caudate ( $F(13,403) = 1.445, p = .136$ ). Similarly, no significant group  $\times$  time interactions were found for either the left or right caudate (for the left,  $F(13,403) = 1.734, p = .052$ ; for the right,  $F(13,403) = 1.335, p = .189$ ).

#### 1.2.4 Voxel-wise analyses of the group $\times$ valence $\times$ time and the group $\times$ time interactions

For the second stage of analysis, voxelwise effects were assessed in a composite dataset consisting of both the young and older adult subjects. A voxel-wise test of the three-way group  $\times$  valence  $\times$  time interaction did not show any significant effects within the striatum. Outside of this region, two clusters showed a significant effect; peak Talairach coordinates were located in the right parahippocampal gyrus [25,-34,-12] and the right cerebellum [17,-53,-12]. Notably, both of these clusters fell near the border of the area of functional coverage; timecourses extracted from these regions were jagged and did not appear to represent a true hemodynamic effect.

A voxel-wise test of the two-way group  $\times$  time interaction yielded two significant clusters within or near the striatum (see Figure 6). A cluster on the left (peak coordinates = [-3,11,4]) appeared to coincide with both a portion of grey matter in the left ventromedial caudate as well as a more dorsal region that coincided with the white matter immediately anterior the caudate. A cluster on the right (peak coordinates = [16,28,12]) was located almost entirely within the lateral ventricle and the surrounding white matter; a single voxel of this cluster overlapped with the right caudate. Average hemodynamic timecourses were extracted from the left and right clusters; results for the older and young adult subjects are shown in Figure 7. Since the valence factor does not contribute to the test of the group  $\times$  time interaction, timecourse data are collapsed across reward and punishment trials. For the left cluster, young adults demonstrated a robust hemodynamic response, while the older adults' signal appeared relatively flat, with a low-amplitude peak coinciding in time with the younger adults' response peak. Timecourses

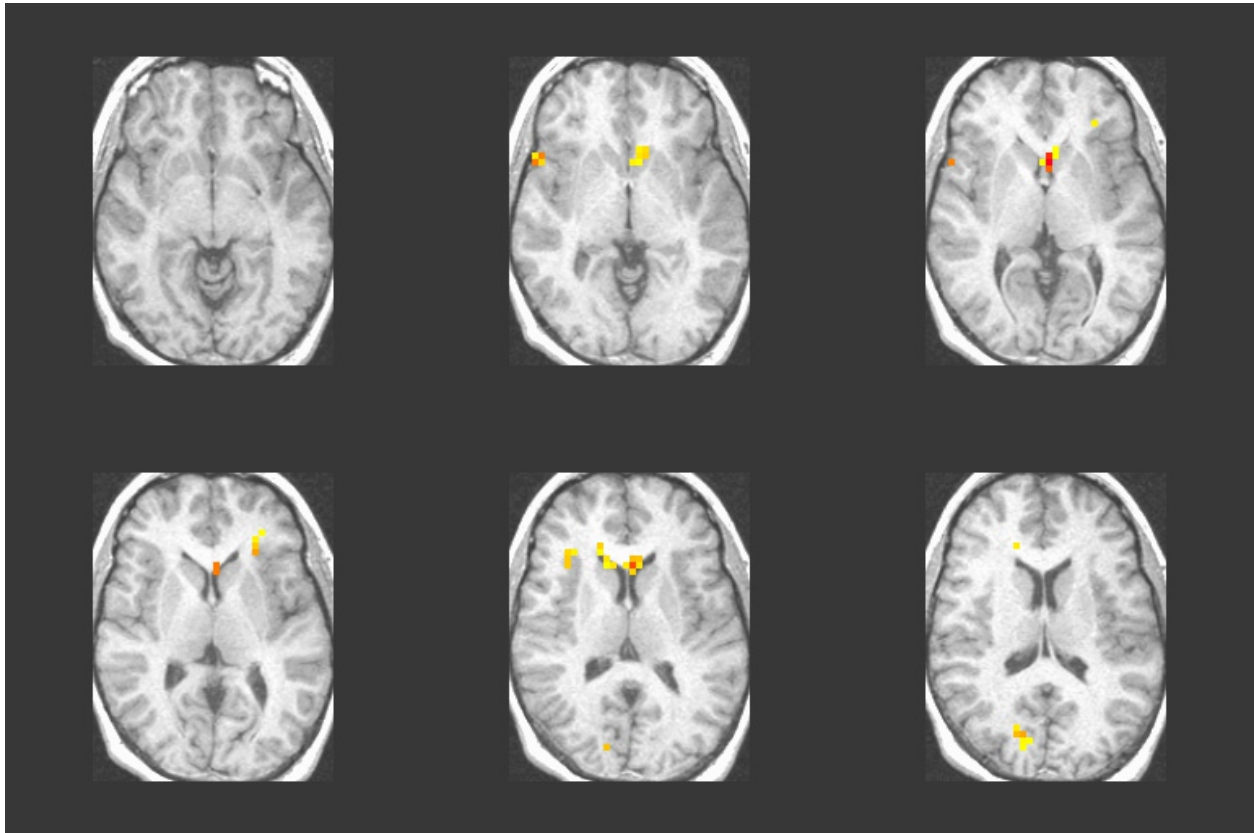


**Figure 6.** Striatal clusters showing a significant group x time interaction at  $p < 0.0001$ , contiguity threshold = 3.

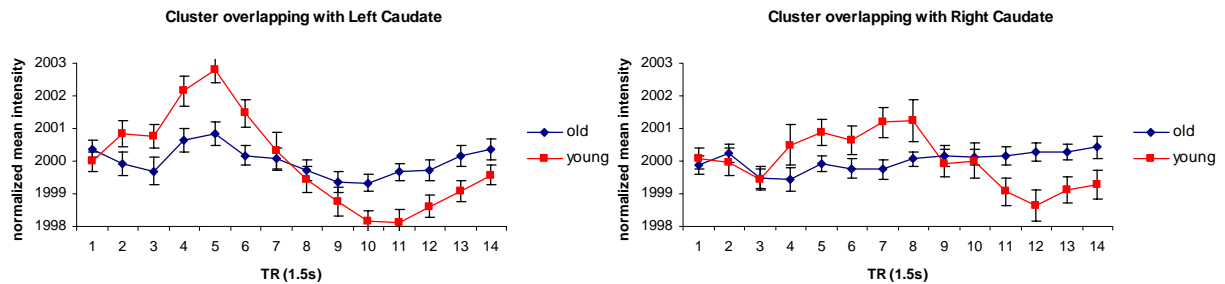


**Figure 7.** Hemodynamic response functions extracted from clusters sensitive to the group x time interaction,  $p < 0.0001$ , cluster threshold = 3 contiguous voxels. The left caudate cluster overlapped with part of the ventromedial caudate as well as surrounding white matter. A single voxel in the right cluster overlapped with the caudate; the remaining voxels fell within surrounding CSF and white matter. Timecourse data are collapsed across valence conditions.

from the right cluster, which fell largely outside of the gray matter, were not as smooth as those extracted from the left. As in the cluster overlapping with the left caudate, the older adults' response was blunted relative to the young adults' response. The shape of these responses was

somewhat unusual, with the peak response in the young subjects not occurring until T8, and the old subjects not showing any discernable peak at all.

Outside of our striatal region of interest, significant group  $x$  time effects were found in twelve other regions; for completeness, the active clusters are displayed in Figure 8 and listed in Table 2. In the majority of these active regions, the young subjects' response profile exhibited a rise in activation followed by a gradual descent to baseline levels; in contrast, the older adults' response was either relatively blunted or flat. (One exception to this observation was found in the middle frontal gyrus, which revealed a robust response for older adults but a nearly-flat response for young adults.) Two sample timecourses are shown in Figure 9, including responses from right cuneus/right BA 18 and from the anterior insula.

It is worth noting that several of the clusters found in the group  $x$  time interaction map are regions that have been observed in previous studies of young adults' activation during the card-guessing task, with responses reported for either the main effect of time (e.g., insula, precentral gyrus, cingulate gyrus, precuneus) or the valence  $x$  time interaction (e.g., lingual gyrus, see Delgado et al., 2000, and Tricomi et al., 2004). The relevance of these extra-striatal regions of age-related effects, in addition to the possible interpretations of the group  $x$  time effect in the head of the caudate, will be considered in the Discussion.

**Table 2.** Functionally-defined clusters of interest sensitive to the group x time interaction,  $p < 0.0001$ , contiguity threshold = 3 voxels.

Location	Peak $F$ value	Peak TT coordinates	Cluster size
Within 1mm of Left caudate	6.76	[-3,11,4]	20
Within 2mm of Anterior cingulate, in white matter anterior to Right caudate	3.96	[16,28,12]	6
Right insula	4.08	[37,20,12]	4
Within 4mm of Claustrum	4.76	[-24,25,8]	5
Right cingulate gyrus/Right BA 32	6.34	[5,25,35]	69
Right precentral gyrus/Right BA 6 (#1)	4.21	[32,-10,54]	6
Right precentral gyrus/Right BA 6 (#2)	4.88	[47,-4,54]	6
Right precentral gyrus/Right BA 4	3.58	[47,-17,39]	3
Middle frontal gyrus	3.84	[-43,6,50]	3
Right superior temporal gyrus/ Right BA 22	5.33	[56,10,0]	5
Right precuneus/Right BA 7	4.91	[6,-72,39]	9
Right cuneus/ Right BA 18	4.67	[14,-76,15]	7
Within 1mm of Right cuneus	5.98	[2,-71,31]	13
Left lingual gyrus/Left BA 23	3.42	[-3,-22,27]	3

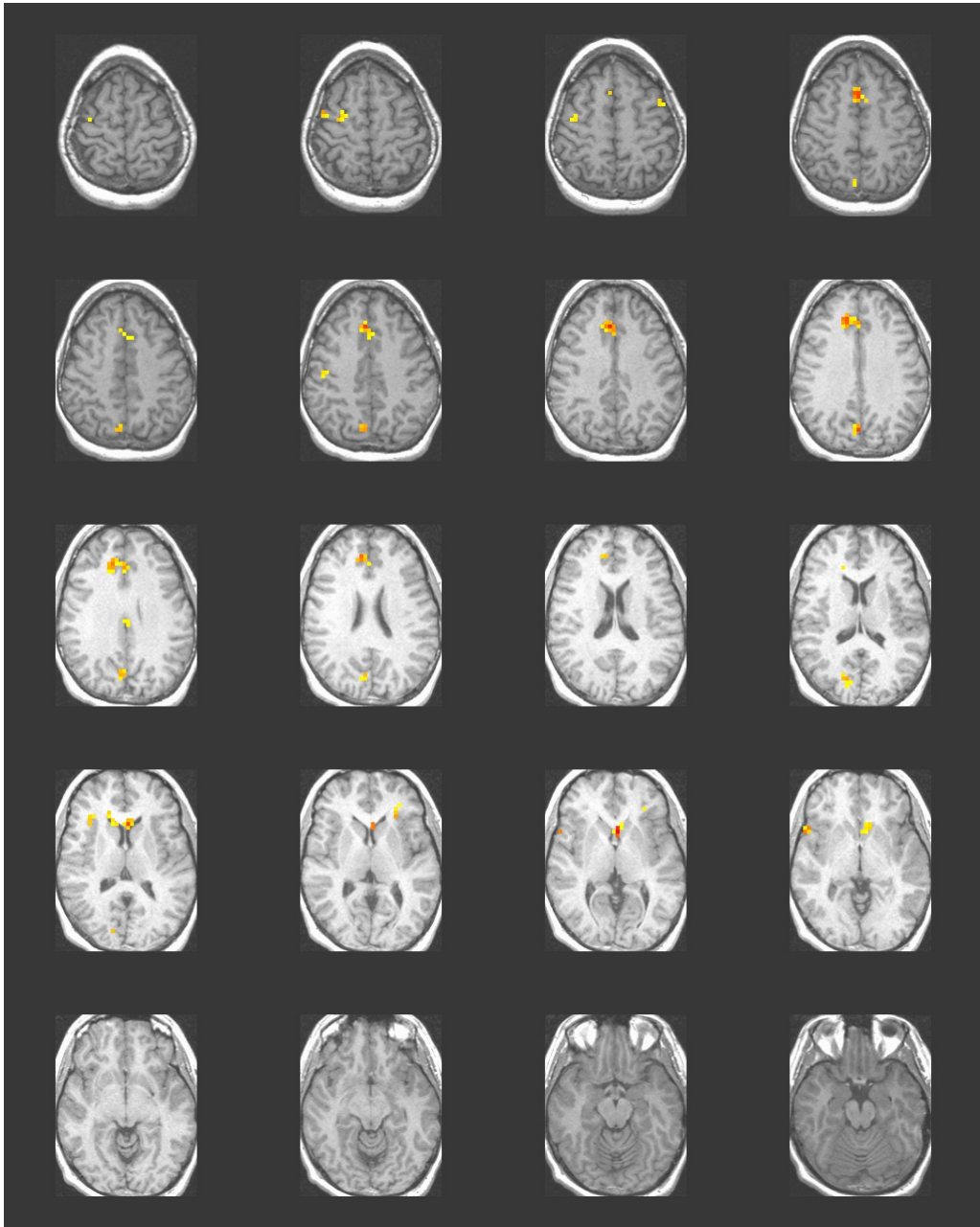


**Figure 8.** Clusters with significant group  $\times$  time interaction effects;  $p < 0.0001$ , contiguity threshold = 3.

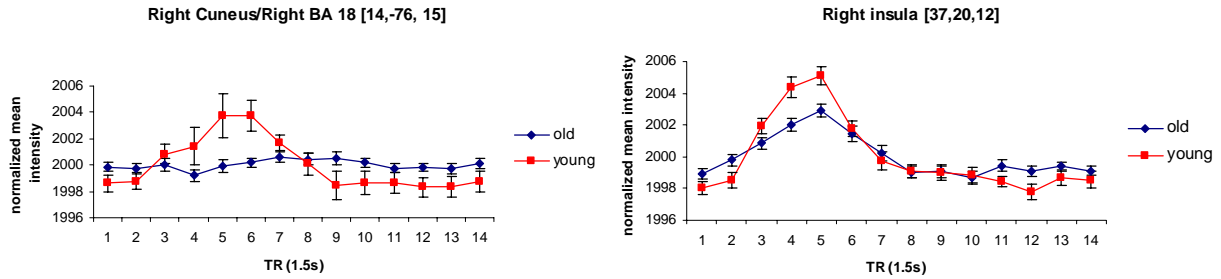


**Figure 9.** Two examples of hemodynamic timecourses from clusters outside of the striatum that showed a significant group x time interaction.

### 1.3 DISCUSSION

The goals of the present study were (1) to establish a valid means of measuring reward- and punishment-related hemodynamic responses in the striatum of older adults, (2) to characterize the temporal profile of the observed responses, and (3) to compare the nature of these responses to those of young adults. To pursue these aims, we scanned older and young adult volunteers as they completed a card-guessing task that has been replicated across a number of previous studies (Delgado et al., 2003; Delgado et al., 2000; Hariri et al., 2006; Tricomi et al., 2004; Tricomi et al., 2006) and has been associated with a well-defined pattern of hemodynamic responses to both reward and punishment outcomes. In order to accommodate some of the common methodological concerns encountered in healthy older adults, we recruited a relatively large number of participants, lengthened the inter-trial interval of the guessing task's slow event-related design, and used a novel high-dimensional co-registration procedure to align subjects' functional data to a local reference brain.

The principal finding of the study is that striatal responses to reward and punishment are

preserved in healthy older adults, with a focus of activation in the bilateral head of the caudate nucleus that closely overlaps with the region that is observed when young adults complete the guessing task. Furthermore, the temporal evolution of the caudate's response to reward and punishment retained one of the most predominant characteristics observed across multiple studies: an enhanced response to rewards relative to punishments during the 6-9 s period following outcome presentation (Delgado et al., 2003; Tricomi et al., 2004). These three positive findings in the older adults -- robust caudate activation, a locus of activity that is consistent with previous studies, and a more sustained response to rewards than to punishments -- provide encouraging evidence that the guessing task may be appropriately applied to the study of reward- and punishment-related processing in healthy older adults.

Of some interest, however, is the fact that older adults' punishment response did fail to show one feature that has been previously reported for younger subjects: A rapid response peak that surpasses the reward response during the 1.5-3 s post-outcome interval (Delgado et al., 2003; Delgado et al., 2000). On the one hand, it is unclear how much significance should be attributed to this null result, especially in light of the lack of any 3-way group  $\times$  valence  $\times$  time interaction effects in the striatum, which would have supported the claim that the relationship between the reward and the punishment responses somehow differs between the two age groups. Furthermore, the early punishment peak is something of a "fragile" phenomenon to measure, given its occurrence during a very short period following the outcome display. On the other hand, both reward researchers and aging researchers (Larkin et al., 2006) have begun to promote the idea that the positivity bias -- a phenomenon that relates healthy aging to a reduced tendency to experience negative affect (Mather & Carstensen, 2005) -- may apply to older adults' perception of punishing events. Consistent with this expectation, a recent unpublished

neuroimaging experiment (Larkin et al., 2006) found that older subjects showed diminished anterior insula responses to the anticipation of a potential monetary loss; furthermore, the older adults tended to report very modest levels of “negative arousal” when faced with the prospect of this negative outcome. Therefore, if one interpreted the early punishment peak in the caudate as reflective of an individual’s subjective experience of aversive events, then it is conceivable that the loss of this peak in the older adults is somehow related to an age-related positivity bias. However, considering that the short duration of the punishment peak may make it particularly susceptible to noise-related factors, such interpretations are very speculative and should await further confirmation that the peak is consistently absent across multiple studies in older adults.

In summary, then, the lack of an early punishment peak in the older adults (and the presence of this peak in the young adults) was the only feature we observed that might indicate a difference in the way that the valence  $\times$  time interaction is expressed in these two populations, and even this difference received only indirect statistical support. The other test performed at the group level – the test of the group  $\times$  time interaction – was used to detect any age-related effects on striatal activity that were not specific to a particular outcome valence. This test was performed on striatal timecourses that were derived in two different ways, with only one of the two methods indicating any significant differences between groups. Initially, we tested for age-related effects on the hemodynamic data extracted from the most-active voxels that were defined for each age group separately. While older adult responses derived in this way appeared slightly blunted relative to those of the young adults (particularly in the left caudate), the group  $\times$  time interaction for these timecourses was not significant. Following this step, we performed a voxelwise group  $\times$  time test on the data from both age groups combined; this test revealed two active clusters that partially overlapped with the bilateral head of the caudate, with additional

voxels extending into the surrounding white matter and cerebral spinal fluid. The “cleanest” group  $\times$  time effect was associated with the larger, left cluster, which demonstrated a marked blunting of the old adult response relative to a fairly robust young adult response.

As in the case of the absent punishment peak, this blunting effect is difficult to interpret. A generalized scaling in the task response is somewhat uninteresting in light of our original question of interest, which emphasized the outcome-specific responses of the striatum. However, it may be worthwhile to gain a better understanding of this blunting effect in the caudate, especially if it may be argued to arise from a fundamentally artificial cause: If the methodological features of this particular study caused this effect to appear, this suggests that our current procedures for implementing the guessing task, while adequate for measuring reward-related responses in older adults, may also be capable of generating false-positive effects in the striatum.

In consideration of this concern, one particular limitation of the current study may be suggested as a possible factor that gave rise to the group  $\times$  time effect in the caudate. An obvious anomaly of the group  $\times$  time activation map was the fact that the active clusters within the striatal region overlapped substantially with white matter and CSF regions within the reference brain. This overlay of functional activity onto white matter and/or CSF was not exclusive to the group  $\times$  time map; a similar spread outside of grey matter boundaries was found in the valence  $\times$  time activation maps for both the young and the old groups (see Figure 4). With the “perfect” co-registration procedure (as well as precise functional overlay in the original space), no true BOLD effects should localize to these regions; however, inspection of single-subjects’ co-registered datasets suggested that the anterior caudate was an occasionally problematic region for the fully-deformable registration procedure (see Appendix A), with the consequence that grey matter

regions from the original structural image were occasionally extended through the most anterior portion of the lateral ventricle. Furthermore, in subjects with particularly pronounced ventricles surrounding the caudate head, the reverse problem was sometimes observed: The ventricles of the warped brain were not sufficiently shrunken to match those of the reference brain.

Therefore, even this powerful co-registration approach appears to be susceptible to the problems introduced by the atrophy present in healthy older adults, and the resulting subtle abnormalities in the warped images may help explain the presence of a blunting effect in a region that overlaps with both the caudate and the nearby CSF. Specifically, one could imagine a scenario in which a single voxel that falls on the caudate/CSF border in the reference brain may include functional data from both young subjects whose grey matter structures were inappropriately warped into that region, as well as from older subjects who are contributing largely CSF-derived responses to that voxel. In this case, the blunting response observed in older adults would be largely due to a disproportionate number of subjects who are contributing ventricle-related, as opposed to grey-matter-related data to the cluster of interest.

While the possibility that the fully-deformable registration procedure resulted in a false-positive age-related effect raises some concerns regarding these small local effects in the striatum, it does not necessarily invalidate the use of this co-registration strategy as a whole. It is unlikely that any spatial normalization procedure is completely impervious to the complicating effects of anatomical variability, and preliminary comparison with a simple 12-parameter affine transformation model (Woods, Mazziotta, & Cherry, 1993) suggests that the fully-deformable model results in superior detection of reliable striatal signals (see Appendix A). The primary implication of the current findings in the CSF and white matter may be that researchers using the fully-deformable procedure should carefully check subjects' warped structural images for even

small anomalies in the final warped result; a failure to account for these effects might result in the incorrect interpretation of an ultimately artifactual effect. Furthermore, this advice may not be restricted to the use of very high-dimensional warping procedures; the tendency to inappropriately align CSF and grey matter regions is likely to be a problem that plagues many co-registration techniques.

It may be somewhat extreme to claim that the blunted caudate effect in older adults is entirely attributable to problems caused by our spatial normalization procedure. Two results suggest that some component of the underlying hemodynamic signal may be truly blunted in the older adult group. First, timecourses extracted from older adults' most active voxels for the valence  $\times$  time effect (which co-localized with the grey matter more consistently) did appear to be slightly blunted; although this trend did not pass the significance criterion of  $p < 0.05$  in either hemisphere, the response in the left caudate was marginally significant ( $p = 0.052$ ). Second, several clusters sensitive to the group  $\times$  time effect were found throughout the brain; while some of these clusters were similarly susceptible to artifactual influences on the signal timecourse (e.g., precentral gyrus, which was located near the dorsal-most border of the area of functional coverage), a number of these regions were not located close to either the ventricles or the edge of the brain. These include the sample regions presented in Figure 9, the cuneus and the insula. In both of these regions – and particularly in the insula --- the responses of both the old and young subjects are reasonably smooth, suggesting that the origin of the effect may be real rather than noise-related. Therefore, the presence of a relatively clean blunting effect in other regions of the brain, many of which have been previously reported to be active during the card-guessing task (Delgado et al., 2000), suggests that a true difference in the hemodynamic signal may contribute

to the group  $\times$  time related effects in the caudate, perhaps in combination with any warping-related effects on the signal.

If older adults' overall response to the card-guessing task is truly blunted, what might this imply? The finding of a reduced response amplitude may not be consistent with an explanation that appeals to fundamental differences in the BOLD signal of older adults, since the basic visuomotor studies conducted in this population have typically not identified strong age-related differences in peak response amplitude (Aizenstein et al., 2004; D'Esposito, Zarahn, Aguirre, & Rypma, 1999; Huettel et al., 2001; Richter & Richter, 2003), particularly when functional clusters of interest are restricted to only the most activated voxels within the older adult group (Aizenstein et al., 2004). A more likely possibility for the generalized blunting is that older adults may have been less engaged in the task as a whole. As was noted in the Methods section, a few participants' sessions were terminated early due to their general discomfort in the scanner; it was not unusual for subjects to make comments regarding back pain, joint pain, or general intolerance of such a long period of stillness in the confined space of a full-body scanner. Factors such as these could have a clear impact on the degree to which older subjects can be engaged in a task that presumably taps into their underlying motivational systems. One improvement in the experimental procedure that might attenuate such discomfort-related effects would be to shorten the duration of the total time in the scanner; a switch from the original slow event-related design of the card-guessing task to a more efficient rapid event-related design may be one step towards preventing the problems that a long period in the scanner environment can create.

None of the group  $\times$  time effects observed in either the striatum or the cortex revealed a hyper-extended hemodynamic response in the older adult subjects. In the overall literature on

the BOLD signal in healthy aging, the slow decay to baseline is a somewhat inconsistently observed effect, with a significant prolongation of the response being reported in some studies (Aizenstein et al., 2004; Richter & Richter, 2003), a marginal or untested effect being observed in other studies (Buckner, Snyder, Sanders, Raichle, & Morris, 2000; D'Esposito et al., 1999), and no apparent effects being seen in the remainder of studies (e.g., Huettel et al., 2001). Therefore, an extended BOLD signal is probably not a feature that is generalizable to the entire population of healthy older adults; perhaps the prolonged response is associated with the severity of some kind of degenerative process that is not necessarily uniform across individuals or brain regions (D'Esposito et al., 2003). Therefore, while no hyper-extension effects were apparent in the current study, it may be worthwhile to keep the potential for this age-related effect in mind when designing future experiments; the lack of a prolonged response in our dataset may simply be due to characteristics specific to our sample (e.g., the relatively young age of our subjects relative to those recruited for studies of “elderly” adults).

In summary, the results of this study suggest the following avenues for future work:

First, the card-guessing task, within the context of our specific design and analysis procedures, appears to offer a valid method for measuring reward- and punishment-related caudate responses in healthy aging. This provides encouraging evidence that this task can be applied to future investigations of reward processing in older adults.

Second, while the older adults exhibit robust differentiation between their striatal responses to rewards and punishments, the early punishment peak observed in previous studies (e.g., Delgado et al., 2003) appears largely absent in this group. However, the lack of a significant age group  $\times$  valence  $\times$  time effect prevents any strong interpretations regarding the

absence of this feature. In future studies, a replication of the reduced punishment peak -- perhaps using analyses with an *a priori* focus on this segment of the response -- would be informative.

Finally, the observation of a generally blunted task response across several regions of the brain is at least consistent with the possibility that older adult subjects were not quite as engaged in the task as the young adult subjects were; a reduced level of engagement could be attributable to various factors that may cause older adults to be somewhat more uncomfortable in the confined space of the scanner. It would be valuable to see if small efforts to improve older adults' experience in the MRI environment could help increase the magnitude of functional effects that are measured when they complete motivation-related tasks. Furthermore, if older subjects completed some kind of self-report measure regarding their experience while they were in the scanner, this information potentially could be used as a basis for excluding data from participants who had extremely negative experiences, or as a covariate in analyses that could control for these factors of overall well-being. If any such procedural or analysis steps resulted in an enhanced effect size of functional responses to reward and punishment, then they might also be usefully applied to attaining the best signal possible in any study that involves an older adult population.

## APPENDIX A

### ALTERNATIVE METHODS FOR SPATIAL NORMALIZATION OF FUNCTIONAL DATASETS: A PRELIMINARY COMPARISON

The well-documented atrophy of both cortical (Raz et al., 2004) and subcortical regions (Raz et al., 1995) in healthy older adults raises questions of how to best align subjects' functional datasets when group-level voxelwise analyses are performed. Of course, it is possible to avoid this need for alignment by extracting region of interest (ROI) data on a single-subject basis. In this case, region definition is determined through the *a priori* selection of specific anatomical regions where task-related activation is expected to be observed.

As a preliminary analysis step in our study of reward-related processing in older adults, we viewed the timecourse of older subjects' responses using anatomical definition of ROIs at the single-subject level. In order to carry out the anatomical ROI method, the boundaries of left and right caudate ROIs were determined based on data from several replications of the card-guessing task in young adult subjects. This approach was useful in that it allowed us some means to extract functional data without relying on the co-registration of older adults' datasets; since data could be derived from subjects' original functional space, the anatomical ROIs provided us with a "ground truth" estimate of how at least a pre-selected subregion of older adults' caudate nuclei responded to rewards and punishments.

Of course, these anatomical ROIs are associated with a clear disadvantage; specifically, it cannot be guaranteed that older adults' region of peak responsiveness to the task is located in the same region that has been functionally-defined with young adult data. To assess older adults' responses in the absence of any predetermined anatomical bias, it was desirable to implement some form of spatial normalization so that group-level voxelwise tests could be performed. The standard procedure employed in our lab – as well as in several previous publications involving the guessing task (Delgado et al., 2003; Delgado et al., 2000; Delgado, Stenger, & Fiez, 2004; Tricomi et al., 2004; Tricomi et al., 2006)— is to align all subjects' data to a single local reference brain using a 12-parameter affine model implemented through the AIR package (Woods et al., 1993). In practice, this low-dimensional linear transformation procedure has the advantage that the specific transformations performed on any single subject's image are relatively transparent; i.e., the nature of the transformation is easy to discern just by viewing the subject's aligned image. The disadvantage of this procedure is its inability to account for finer-level differences between the subject's brain and the reference brain; this shortcoming of the linear model suggests that it may not perform well when registering images that exhibit a high degree of anatomical variability.

Given this possible weakness of the linear model, we conducted an initial analysis in which we compared our standard co-registration approach with a high-dimensional, nonlinear approach. Older adult data that had been processed with the linear transform were compared to the same dataset after it had been processed with a novel fully-deformable co-registration procedure (Wu, Carmichael et al., 2006; Wu, Mazurkewicz et al., 2006). These methods were evaluated using a two-stage process. First, we chose a predetermined region of the brain – the bilateral anterior caudate region identified from our previous data in younger subjects – and

asked how effectively each method was able to align the functional effects associated with this region. Specifically, using a “ground truth” measurement derived from ROIs traced in each individual’s space, we were able to confirm that a reliable group  $\times$  time interaction was present in this region of the older adults’ caudate; these ROIs were then traced on the reference brain that was used for both the linear and fully-deformable co-registration procedures. We subsequently used the ROIs drawn in the space of the reference brain to extract functional timecourses from the full group of subjects that had been registered to this template; for each co-registration procedure, we calculated a measure of reliability ( $F$  values) of the valence  $\times$  time effect expressed by these timecourses. Thus our first-stage evaluation of the two spatial normalization procedures was based on the reliability of the functional effects that were generated within a region of predetermined location and size. This evaluation was based on the assumption that the procedure that more effectively aligned the anatomical area of interest would also yield more reliable functional effects in that area.

The co-registration model that produces the most reliable effects for the focused anterior caudate ROI might also be assumed to be the most effective model for detecting functional effects throughout the striatum. To test this assumption, the second stage of the methods comparison involved a voxelwise test of the valence  $\times$  time interaction in the two co-registered datasets (the same test as was reported in section 1.2.2 of the thesis text). This second stage of the analysis more closely mirrored the way in which these data would be analyzed in practice, since the primary advantage of co-registration is to allow for data-driven, bias-free detection of the most active voxels. The activation maps produced by the voxelwise analyses were compared with respect to the spatial extent of activation and the reliability of the valence  $\times$  time effect in the individual active voxels.

## **A.1 METHODS**

### **A.1.1 Participants**

The same set of twenty older adult subjects who completed the card-guessing task also contributed to this methods comparison.

### **A.1.2 Acquisition and preprocessing of functional data**

Functional data used in the comparison were derived from the eight runs of the card-guessing task that were completed by each of the twenty older adult subjects (with the exception of two participants who contributed only 6 and 7 runs, respectively; see Participants section in the main body of the text). Functional volumes were preprocessed according to the same procedures described for the main experiment.

### **A.1.3 Manual tracing of single-subject ROIs**

Data from five previous studies using the card-guessing task in young adult samples (Delgado et al., 2003; Delgado et al., 2000; Delgado et al., 2004; Tricomi et al., 2004; Tricomi et al., 2006) were used to locate the caudate subregion that had been reliably activated by this task in the past. For each study, the activation map for the valence  $x$  time effect was thresholded at  $p < 0.001$  with a cluster threshold of three significant voxels. These thresholded maps were then overlaid onto the reference brain used in the first publication of the guessing task (Delgado et al.,

2000); the resulting “overlap map” (Figure 10) was color-coded to indicate the number of studies in which each voxel showed a valence  $\times$  time effect.

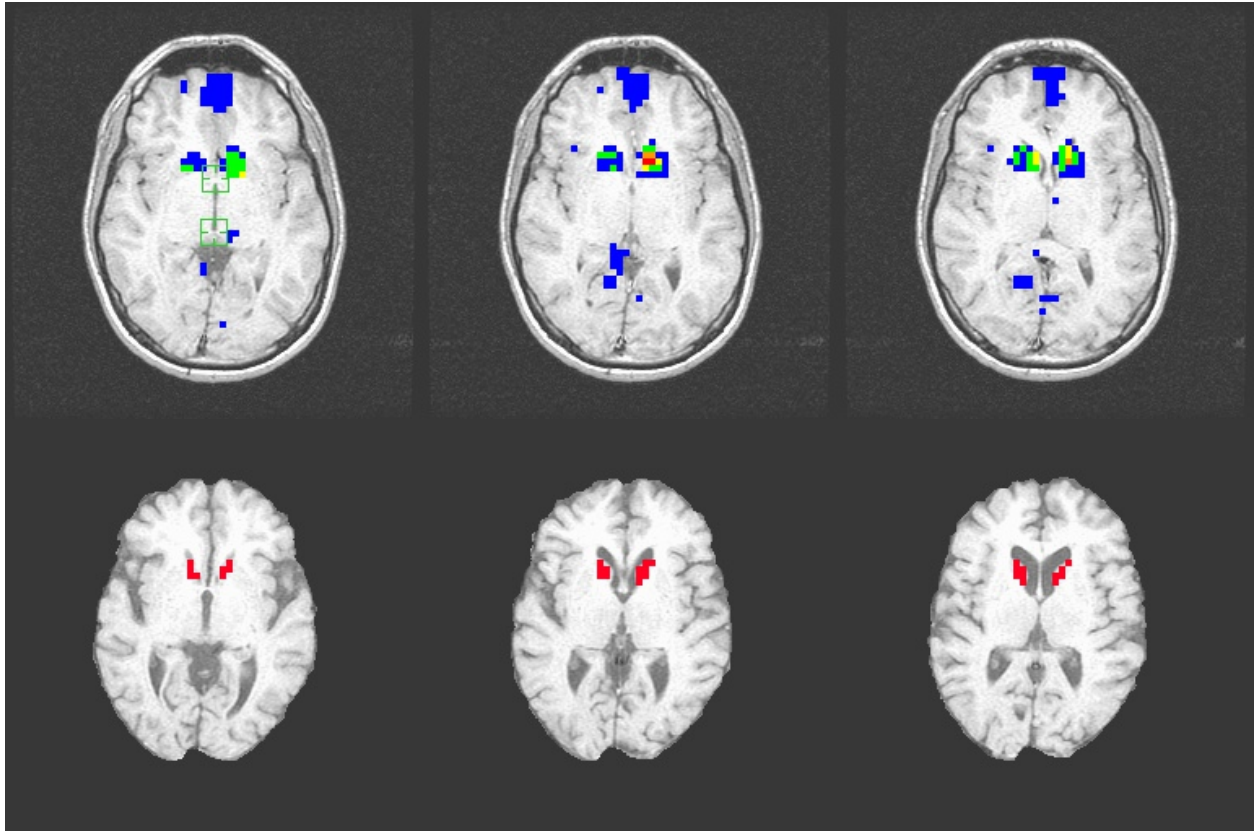


**Figure 10..** Top panel: Valence  $\times$  time maps from five different studies using the guessing task were overlaid on a single reference brain. Green squares mark the anterior and posterior commissures. Colors indicate the number of studies in which a particular voxel was activated (Blue = 1, Green = 2, Yellow = 3, Orange = 4, Red = 5). This overlap map identified a consensus cluster of activation which was then used to guide our placement of manually-traced ROIs. An example of these ROIs for a 66-year-old female is shown in the bottom panel.

The overlap map revealed two voxels in the left caudate where a valence  $\times$  time effect was present in all five studies, and a more extensive bilateral region where voxels of common activation were shared across three or more studies. These clusters of converging activation were used to define a three-slice region of interest that was manually-traced on all individual subjects' low-resolution structural scans. Specifically, ROIs for each subject were traced within the boundaries of the caudate grey matter on the slice containing the superior edge of the anterior commissure, and on the two slices immediately dorsal to that landmark. Traced ROI regions

were then downsampled to the resolution of the functional image (3.8 x 3.75 x 3.75mm voxels) so that average functional timecourses could be extracted.

#### **A.1.4 Co-registration with an affine model**

Consistent with the approach described in previous reports of the card guessing task (Delgado et al., 2000), the low-resolution inplane structural images from each subject were transformed to a common reference space using the 12-parameter affine model of the AIR ‘alignlinear’ program (Woods et al., 1993). The reference image used for co-registration was the structural inplane image collected from a 29-year old subject who had not contributed to the current functional dataset. Each transformed image was viewed in order to confirm that no gross errors in registration had occurred. To illustrate the results of the AIR affine transformation for brains that might be relatively challenging to co-register, the original structural images and the transformed images for the three oldest participants are shown in Figure 11.

The transformation defined for each subject’s structural image was applied to all functional volumes. The co-registered functional images were then submitted to the same intensity normalization and spatial smoothing steps described in section 1.1.4 of the main text.

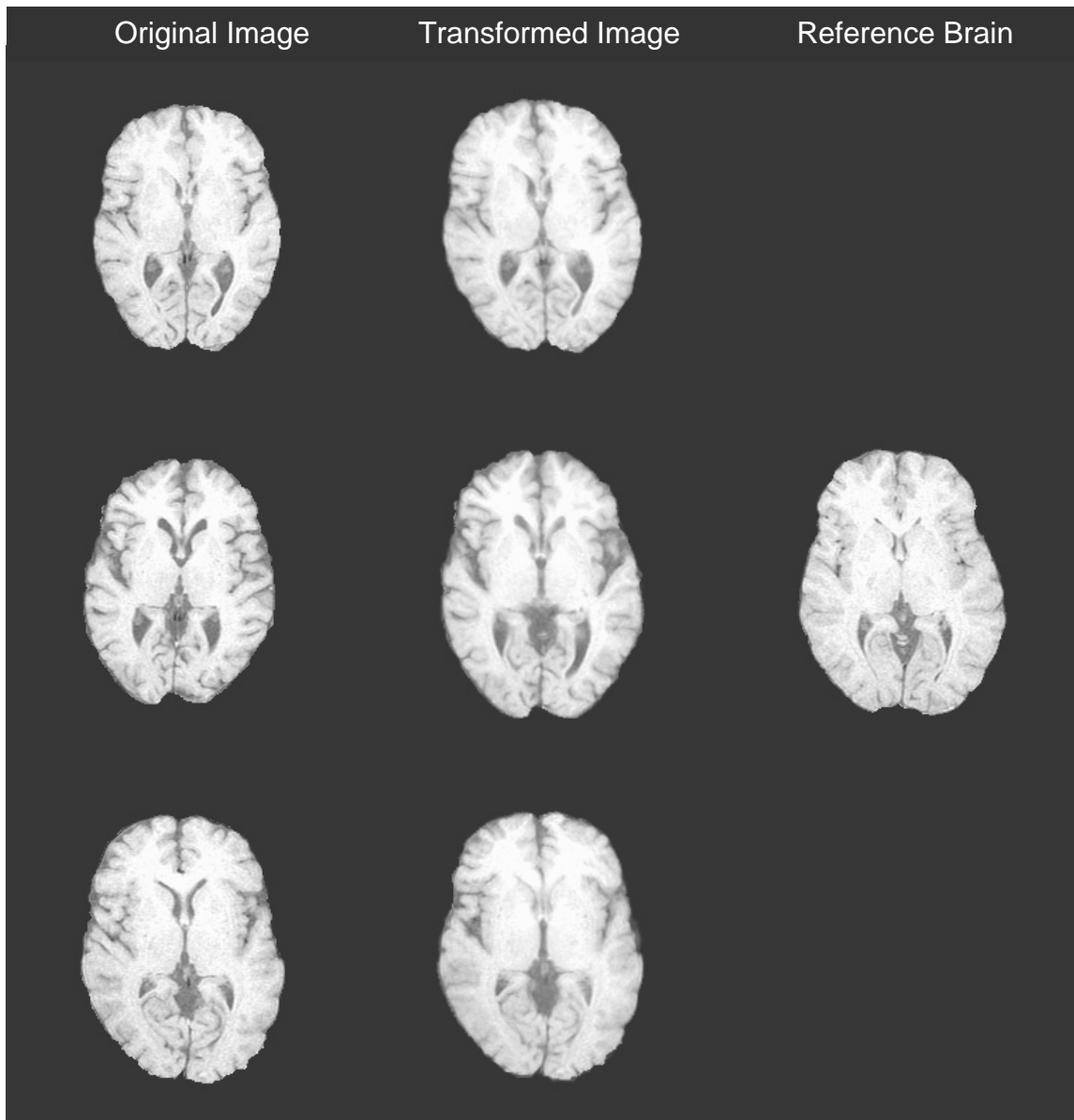


**Figure 11.** Original (left) and transformed (center) structural images for the three oldest subjects in the sample. The reference image is shown on the right. First row, female/64y, second row, female/66y, third row, male/68y. The reference brain is a male, 29y.

### A.1.5 Co-registration with a fully-deformable model

The linear co-registration model was compared with a second, fully-deformable model based on algorithms from the Insight Segmentation and Registration Toolkit (ITK). The fully-

deformable registration procedure has been previously reported as a promising method for warping a standard anatomical atlas (i.e., an atlas drawn on the ‘colin27’ brain) to individual structural images (Wu, Carmichael et al., 2006); the reader is referred to this report for more specific details of the underlying algorithms, as well as a demonstration that this approach can produce results superior to those found with nonlinear approaches from other packages (e.g., AIR (Woods et al., 1998) and SPM (Friston et al., 1995); see also Wu, Mazurkewicz et al., 2006).

The fully-deformable approach was procedurally somewhat more complex than our standard co-registration procedure, with the entire process requiring a number of steps. Each subject's high-resolution SPGR image was first aligned to the reference brain using the same 12-parameter affine model described above; these aligned images were then warped using the fully-deformable procedure. The warps defined for the structural images were then applied to functional datasets which had been upsampled to have the same resolution as the SPGR (1mm cubic voxels). Prior to statistical analysis, the warped functional images were downsampled to their original resolution. These downsampled images were then normalized and smoothed. In order to allow for overlay of the functional data onto the anatomy, the reference SPGR was also downsampled to have the same voxel depth as the functional images (down to .9375 x .9375 x 3.8 mm, the same resolution as the structural inplanes).

Each warped SPGR image was viewed to confirm that no serious errors in registration had occurred (e.g., displacement or gross distortion of the anatomy). Sample warps for the three oldest subjects in the sample are shown in Figure 12. Special attention was paid to the quality of the warp in the vicinity of the striatum. As can be seen in the figure, no serious distortion of

the nuclei were observed; however, it is worthwhile to note some subtle effects. First, for some subjects with a particularly pronounced gap at the anterior tip of the lateral ventricle (see second

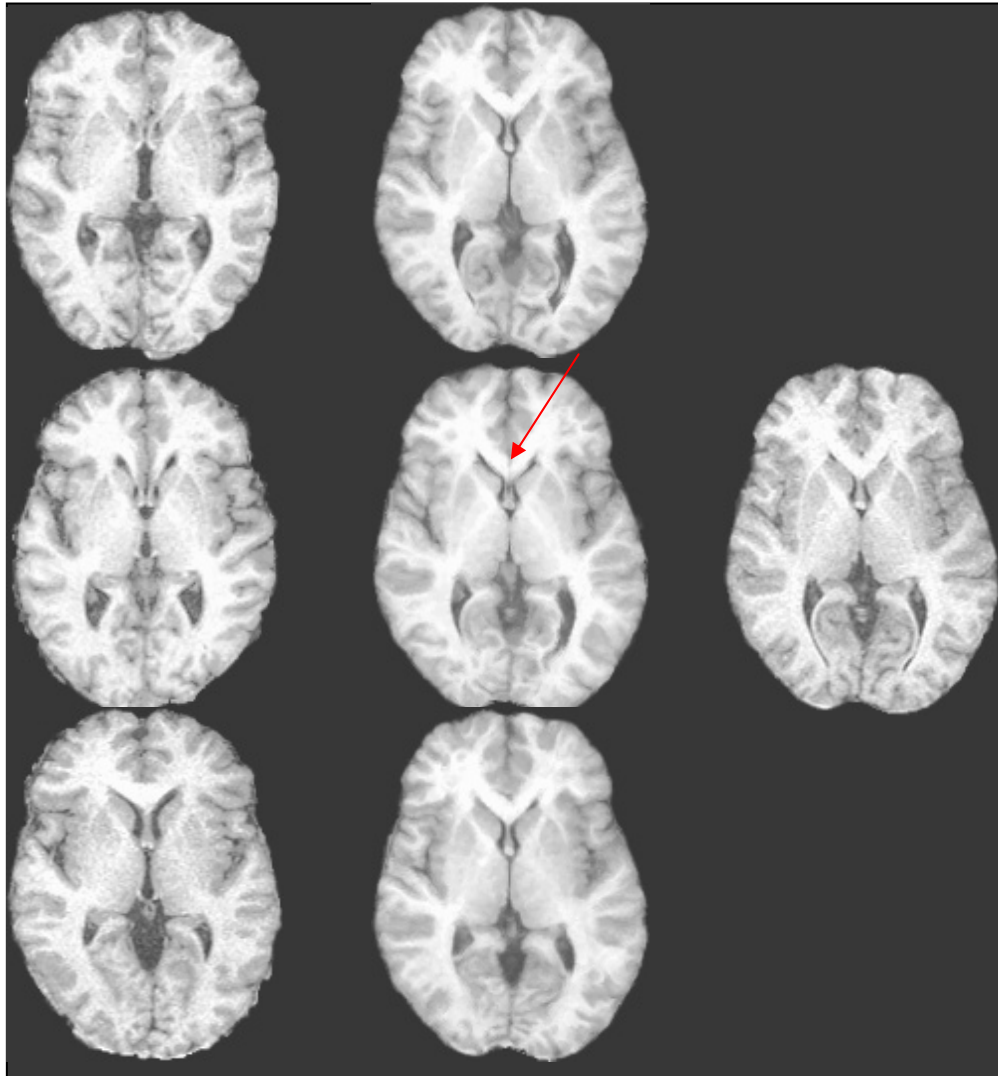


**Figure 12.** Original (left) and warped (center) high-resolution structural images for the three oldest subjects in the sample. The reference image is shown on the right. Red arrow indicates a CSF-related “gap” in the warped subject that was not present in the reference brain.

row of Figure 12), the warping algorithm failed to completely “close-up” this gap. A second small anomaly in some of the warped images was seen in the subject in the top row of Figure 12 and is further illustrated in Figure 13. Specifically, in some individuals for whom this anterior-

most extreme of the lateral ventricle was very thin or entirely absent, the warping procedure appropriately widened this CSF region but also appeared to “smear” some of the caudate grey matter into this area as well.



**Figure 13.** Illustration of a small distortion of the anterior caudate by the fully-deformable co-registration. Subject is a 64 year-old female also shown in the top panel of Figure 12. Notice the spread of the grey matter across the lateral ventricle. This is most apparent on the left side of the brain (right side of the image).

### **A.1.6 Statistical analysis of the functional data**

Evaluation of the linear and fully-deformable methods consisted of two stages. The first analysis compared the two methods on their ability to generate a reliable valence  $\times$  time effect in the bilateral caudate region of interest that was described in section A.1.3. To confirm that older adults did express a significant interaction effect in this region, average timecourse data were extracted from the ROIs that had been drawn in single-subject space and submitted to the timecourse normalization procedure described in section 1.1.5 of the main text. The resulting left and right caudate timecourses were tested with a 2-way repeated measures ANOVA with valence and time as factors. To examine this same effect within the co-registered datasets, the

caudate ROIs were also traced on the reference brains that had been used for the two registration methods. In the case of the linear method, these tracings were done on the reference subject's low-resolution structural image; in the case of the fully-deformable method, the ROIs were drawn on an SPGR which had been downsampled to the same resolution as the low-resolution image. Although these two brain images were derived from the same subject during a single scanning session, the nature of their acquisition was such that their exact positioning within the voxel matrix was slightly different, with the result that ROIs drawn on these two images were also slightly different but were constrained to contain the same number of voxels.

The ROIs traced on the reference brain were resampled to the coarser resolution of the functional space; these regions were then used to obtain hemodynamic timecourse information from the full group of co-registered subjects. The resulting average timecourses were then normalized and submitted to the same valence  $\times$  time test described for the single-subject ROIs.

The purpose of the second stage of analysis was to compare the voxelwise effects generated by the two different registration methods. Therefore, the same valence  $\times$  time interaction effect was tested on a voxelwise level for each dataset. The resulting statistical maps were thresholded at  $p < 0.0001$  with a cluster threshold of 3 voxels (note that for the fully-deformable procedure the results of this test also appear in the main body of the text). For each method, the spatial extent of activation within the striatum was noted, as well as the  $F$  value for the peak active voxel.

## A.2 RESULTS

### A.2.1 Confirmation of a valence $\times$ time effect in the caudate ROIs

Hemodynamic data from the caudate ROIs drawn in single-subject space confirmed that this region was associated with a significant valence  $\times$  time effect in older adults (for the right,  $F(13,247) = 3.364, p < 0.0001$ ; for the left,  $F(13,247) = 3.422, p < 0.0001$ ).

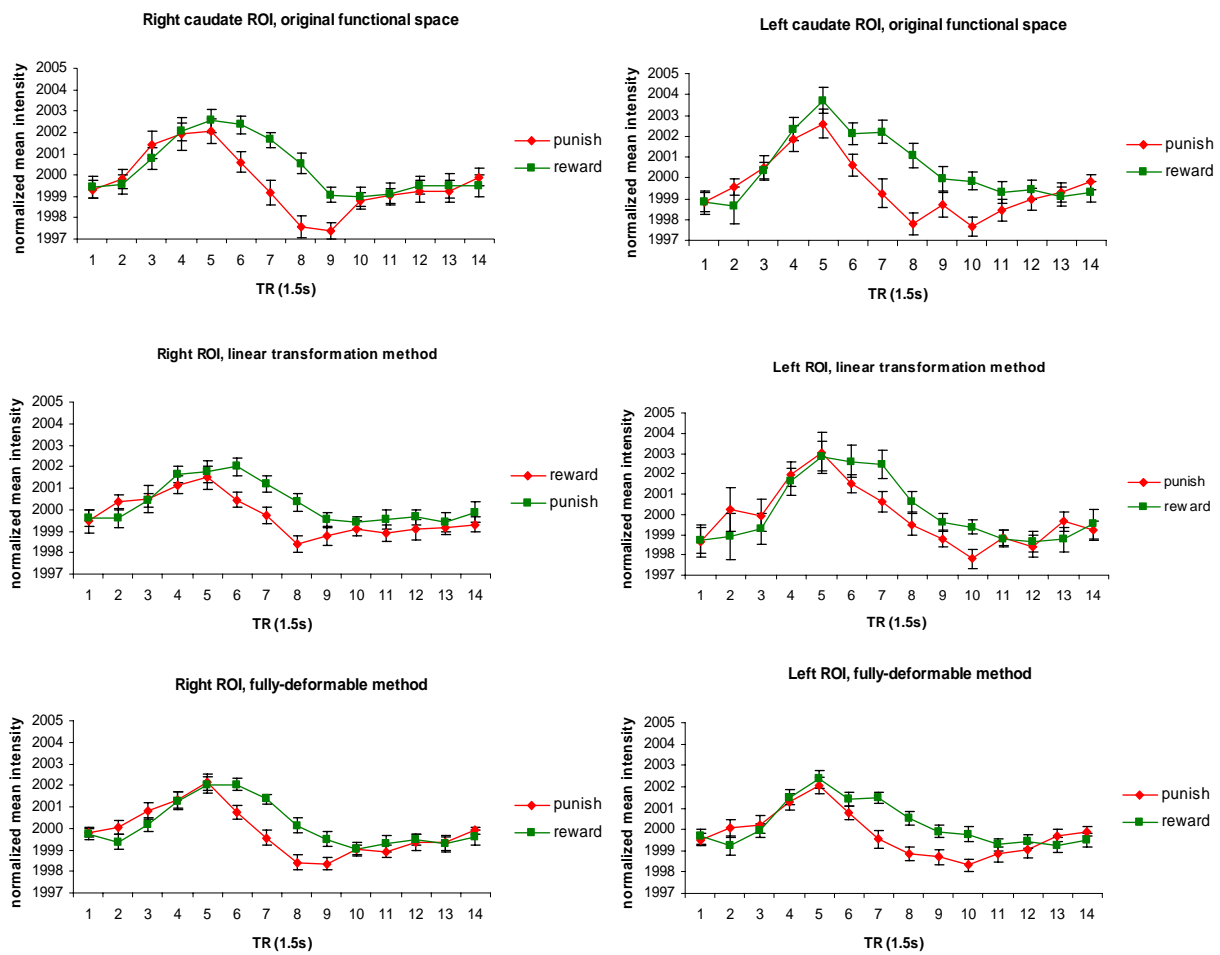


**Figure 14.** Average hemodynamic response functions extracted from a manually-traced bilateral region in the anterior caudate. Top row: ROIs traced in the individual subjects' original functional space. Second row: ROIs traced on a reference brain to which all subjects had been registered with a linear model. Third row: ROIs traced on a reference brain to which all subjects had been registered with a fully deformable model.

Timecourses from the right and left ROI's are shown in the top row of Figure 14. The responses in these two regions generally reflected the expected caudate response, with a more sustained response to reward than to punishment.

The hemodynamic data extracted from the co-registered datasets are presented in the second and third rows of Figure 14. The similarity of the timecourses produced by the two methods was visually compelling; however, the underlying reliability of the interaction effect was quite different. For the linear registration method, the valence  $\times$  time effect reached only a modest statistical threshold (for the right,  $F = 2.198$ ,  $p = .010$ ; for the left,  $F = 1.972$ ;  $p = .024$ ). For the fully-deformable method,  $F$  values were considerably higher (for the right,  $F = 4.527$ ,  $p < 0.000001$ ; for the left,  $F = 3.869$ ,  $p < 0.0001$ ). Thus, it seems likely that the fully-deformable method most effectively aligned the functional responses associated with this restricted region of the anterior caudate.

Similarly, voxelwise tests revealed that fully-deformable registration was associated with a greater spatial extent of striatal activation than was observed for the linear registration approach. Activation maps for the two methods are shown in Figure 15. Data warped with the fully-deformable method yielded extensive bilateral activation, with 21 active voxels that coincided with the grey matter of the caudate. In contrast, data aligned with the linear method produced only a small cluster of activation (5 active voxels) overlapping with the right caudate and nearby putamen. Not surprisingly, the peak  $F$  values recorded for the active clusters were greater for the fully-deformable method (for the left,  $F_{\max} = 4.17$ ; for the right,  $F_{\max} = 5.15$ ) than for the linear method (for the right,  $F_{\max} = 3.98$ ). Timecourses extracted from the left and right active clusters from the fully-deformable method are shown in the main text (see section 1.2.3);

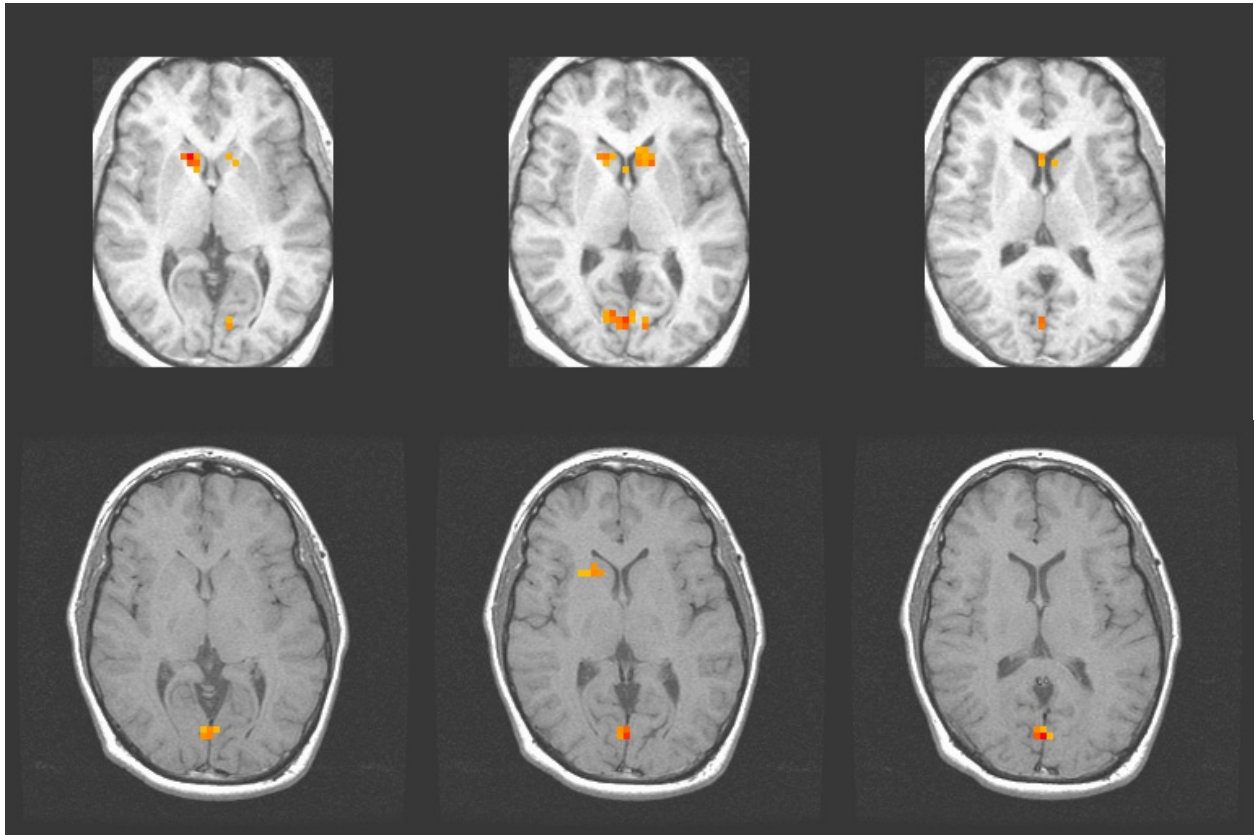


**Figure 15.** Spatial extent of activation for the fully deformable (top) and linear (bottom) co-registration methods. Activation maps show the valence  $\times$  time interaction effect thresholded at  $p < 0.0001$  with a cluster threshold of 3 contiguous voxels.

the timecourse from the single region detected with the linear co-registration method is shown in Figure 16. One interesting trend in this timecourse is the early punishment peak that precedes the reward response peak; this feature of the punishment response has been frequently observed in previous studies of the card-guessing task (Delgado et al., 2003; Delgado et al., 2000; Tricomi et al., 2004) but was largely absent in the older adult timecourses produced by either the fully-deformable registration method (see section 1.2.3) or the anatomical ROI method (see Figure 14).

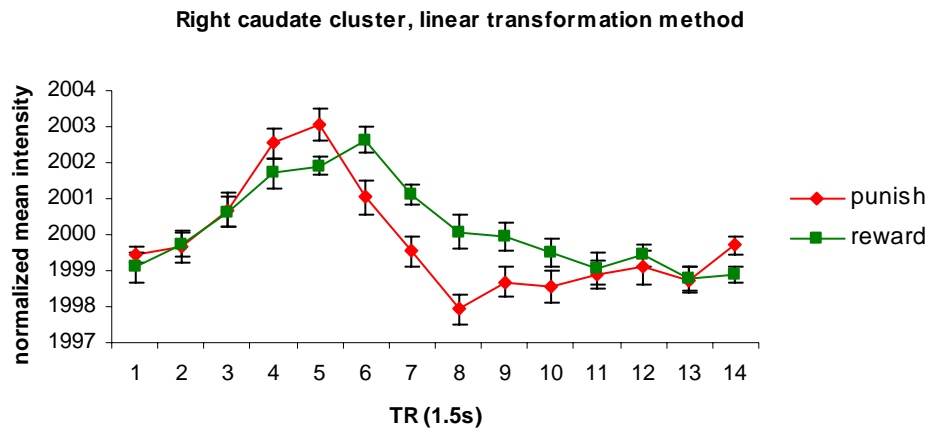


**Figure 16.** Hemodynamic response function for a significant striatal cluster identified by the linear transform procedure. The cluster overlaps with the right anterior caudate and nearby putamen.

### A.3 DISCUSSION

Preliminary tests provided evidence suggesting that a novel, fully-deformable co-registration procedure might be an especially effective tool for detecting reliable signals in the present older adult dataset. Relative to our standard procedure based on a 12-parameter affine model, this new high-dimensional approach was able to produce both a more reliable functional effect within a predetermined anatomical region as well as a greater spatial extent of activation as assessed by voxelwise tests.

It should be noted that this methods comparison was an informal test conducted to inform our own decision for the current study, and was not optimally-designed to allow inferences about how these methods might perform for other studies or subject samples. Several limitations of the present analysis can be identified. First, a study that would allow one to generalize the results of a methods comparison to an entire hypothetical population of similar studies would require some kind of inferential statistics to confirm that a method superiority effect is significant; we used no such statistical tests to directly compare the two registration methods. A formal test of these

methods would necessarily involve some kind of datapoint that could be measured across multiple instances--i.e., a value of registration quality that is calculated for each subject, or a value of functional effect size that is calculated for each of multiple studies conducted to evaluate the two methods—so that an error term could be calculated for the statistical test. Second, the two registration procedures would be more fairly tested by using the same structural image (e.g., the high-resolution SPGR) for each approach; the choice of the low-resolution image for the linear approach was based simply on precedent and convenience. While the use of high-resolution SPGR data would probably not greatly improve the performance of a linear algorithm, it would at least remove one handicap associated with the linear procedure in the current study.

While the evidence in favor of the fully-deformable model was encouraging, the presence of some small anomalies in the warped images should be kept in mind when interpreting any functional data registered with this approach. Within the region of the striatum, the anterior contour of the lateral ventricle surrounding the caudate appeared to be a particularly challenging region for the warping procedure to negotiate. Therefore, any functional effects detected at this caudate/CSF border might be due to an artifact of the warping procedure, and not to a true hemodynamic effect. (This issue is further considered in the Discussion.) It may be worthwhile to explore how varying the specific parameters of the fully-deformable approach (e.g., the width of the smoothing kernel) might affect how the algorithm manages these challenging areas of the brain.

Finally, these preliminary comparative analyses were all conducted with an exclusive focus on effects in the striatum. Given that the guessing task does not consistently activate any region outside of the striatum (with the exception, perhaps, of some poorly-understood regions in occipital cortex), this task did not provide the opportunity to study how effectively the fully-

deformable procedure aligns the functional effects associated with specific cortical regions.

Given that cortical areas are not defined by such well-demarcated boundaries as the basal ganglia are, the cortex may pose a number of difficulties to a high-dimensional warping procedure, thus suggesting it may be a worthwhile focus of future tests of the fully-deformable model.

## **APPENDIX B**

### **STRIATAL ACTIVATION IN OLDER ADULTS DURING A BASIC VISUOMOTOR TASK: THE FINGER-TAPPING EXPERIMENT**

As part of our investigation of older adults' striatal activity during the guessing task, one aim was to identify how the shape of their hemodynamic responses to reward and punishment might differ from those observed for younger adults. The finding of age-related effects on the hemodynamic response function would potentially have both methodological and theoretical implications for future studies on reward-related processing in healthy aging. From an analysis standpoint, a response shape that varies as a function of aging may call into question the use of a canonical hemodynamic response function (e.g., Cohen, 1997) to model older adults' striatal activity. However, on the basis of data from the card-guessing task alone, it is not clear if this implication for data analysis would apply only to contexts involving some kind of incentive processing, or to any task that robustly engages the striatum. Similarly, the data from the card-guessing task might do little to constrain hypotheses on how reward-related processing might function in the aging brain. A change in the temporal dynamics of the striatal BOLD signal might reflect altered neuronal activity (implying an altered neurobiological substrate to reward processing), or it may simply reflect an altered coupling between cell firing and the hemodynamic response (D'Esposito et al., 2003). In the latter case, any shape differences found

in striatal responses should be task-independent and found even for basic visuomotor tasks, which activate the sensorimotor region of the putamen (Lehericy et al., 1998).

While this question regarding the generalizability of age-related hemodynamic effects was beyond the scope of our primary study using the guessing task, it is a question of obvious interest to the larger community of researchers who study either healthy aging or reward processing. For this reason, we added twenty-four trials of a bimanual finger tapping task (Aizenstein et al., 2004) to our experimental protocol so that we could examine striatal responses for subjects who had completed both our card-guessing task as well as a basic visuomotor task. The addition of the finger-tapping task allowed for a preliminary assessment of whether or not aging effects on the striatal BOLD signal generalize across task demands.

## **B.1 METHODS**

### **B.1.1 Participants**

All of the older adults and young adults who completed the card-guessing task (see Section 1.1.1) also completed the finger-tapping task during the same scanning session. One older adult subject with excessive head movement that occurred only during the finger-tapping portion of the experiment was removed from the analyses for this task. Thus the final set of subjects analyzed for the tapping task included 13 young adults and 19 older adults (for the old group, mean age  $\pm$ SD = 57.74 $\pm$ 4.712).

### **B.1.2 Finger-tapping task**

A bimanual finger-tapping task has been utilized previously to investigate aging effects on the BOLD signal in visual and motor cortex (Aizenstein et al., 2004). Subjects were presented with two runs of this task with 12 trials per run. The software and apparatus used for administering this task were the same as those described for the card-guessing task (Section 1.1.2) with the exception that subjects used response units on both the right and left hands. Response and reaction time data were logged for each hand.

As in the case of the card-guessing task, the finger-tapping task is based on a slow-event related design. A trial began with the presentation of the word “TAP” in the center of the screen for 1.5 s. Subjects responded to this cue with a single bimanual button-press using their left and right index fingers. While subjects were instructed to respond “as soon as” they saw the cue appear, the response was not emphasized as a speeded one. The “TAP” display was followed by a variable inter-trial interval consisting of 16.5-19.5 s of fixation.

All subjects read written instructions for the finger-tapping task and completed four trials of practice before entering the scanner.

### **B.1.3 fMRI data acquisition**

Functional data collected during the finger tapping task were acquired using the same parameters and slice prescription described in section 1.1.3 of the main text. Altogether there were two runs of functional acquisition, with each run lasting 4 min and 1.5 s.

#### **B.1.4 Preprocessing of functional data**

The raw data were preprocessed using the same procedures described in section 1.1.4.

#### **B.1.5 Statistical analysis of functional data**

As in the case of the card-guessing task, the timing parameters used for the tapping task allowed for two potentially valid methods of estimating the hemodynamic response. Under the assumption that the response returns to baseline within the minimum 16.5 s fixation interval, timecourses for each subject can be determined by averaging the first 18 s of each trial (or with a TR of 1.5 s, the first 12 scans); data from extra timepoints (i.e., T13-T14) are discarded in this analysis. If responses do not return to baseline within this interval, hemodynamic timecourses can be estimated by submitting the full jittered dataset to a GLM-based deconvolution algorithm (e.g., AFNI 3dDeconvolve (Cox, 1996)) that does not assume a standard response shape. Similar to our observation with the guessing task, responses to the tapping task did appear to resolve within the minimum 16.5 s fixation period, thus supporting the assumptions of the simple averaging approach. Therefore, for each voxel and each subject, average intensity values were computed for the first 12 timepoints of each tapping trial. These subject-level averages were then submitted to group-level statistical analyses.

Analysis of the functional data consisted of two stages that mirrored the analyses performed on the card-guessing task. For the initial set of analyses, data from the older- and young-adult subjects were divided into two separate datasets so that voxel-wise definition of clusters of interest could be determined independently for the two age groups. This step allowed for the comparison of age-related differences for timecourses that had been derived from the

most reliably active voxels in each group. To detect these active voxels, a separate one-way repeated measures voxelwise ANOVA was performed within each age group, with time (an index of the 12 scans in each trial, T1-T12) as the only factor. These analyses were performed with an *a priori* focus on the striatum and in particular the sensorimotor region of the putamen. Activated voxels were identified as those that demonstrated a significant main effect of time at  $p < 0.0001$ . In order to protect against Type-I errors, a contiguity threshold was applied to each activation map in order to define reliably activated regions of interest (Forman et al., 1995). Minimum cluster sizes were determined using the AFNI AlphaSim program (Cox, 1996) such that a significant cluster was associated with a corrected  $p$  value of  $< 0.05$ . For the older adult group, this procedure identified a contiguity threshold of five voxels; for the young adults the threshold was set at four voxels. Following the identification of activated clusters, statistical maps were converted into the standard atlas space of Talairach and Tournoux (Talairach & Tournoux, 1998) in order to determine the anatomical focus of each cluster of interest.

The statistical maps generated by the separate-groups analysis could then be used to qualitatively compare the general distribution of putamen activation in the older versus the young adult subjects. Since we report in the Results (section B.2.2) that we did not find any overlapping significant clusters between the two age groups, we did not perform any direct comparisons of the hemodynamic timecourse data associated with the young and older adult clusters.

For the second stage of analysis, older and young adult data were combined so that voxelwise analyses could be performed on a composite dataset. To test for age-related effects, the full set of functional data were submitted to a 2-way mixed voxelwise ANOVA with group

and time as factors. Statistical maps for the group  $\times$  time interaction were thresholded at  $p < 0.0001$ , with a cluster threshold of three significant voxels as determined by AFNI AlphaSim.

## **B.2 RESULTS**

### **B.2.1 Behavioral results**

Due to a technical error, behavioral data were lost for a single older-adult subject. For the remaining subjects, reaction time analyses were performed on the first button press detected on each trial (i.e., the button press from the hand that responded most quickly). An independent samples  $t$ -test did not find a significant difference between older and young adults' reaction times for the finger-tapping task (mean  $\pm$  SE = 534.10 $\pm$ 31.01 for old, 500.53 $\pm$ 41.09 for young;  $t(29) = -.665$ ).

### **B.2.2 Sensorimotor striatum activation in older and young adults**

For the first stage of analysis, voxelwise effects were assessed in the two age groups independently. At the  $p < 0.0001$  threshold (see Figure 17), voxelwise analysis of the older adult dataset identified a small cluster in the left putamen (peak Talairach coordinates = [-18,3,12]) as well as a right putamen cluster that was contiguous with a nearby cluster in the bilateral thalamus. To determine if an active cluster could be isolated to the right putamen, the threshold was raised to  $p < 0.00005$ . This more stringent threshold identified a cluster that was restricted to the right putamen [20,11,8]; however, the left putamen cluster was not significant at this threshold.

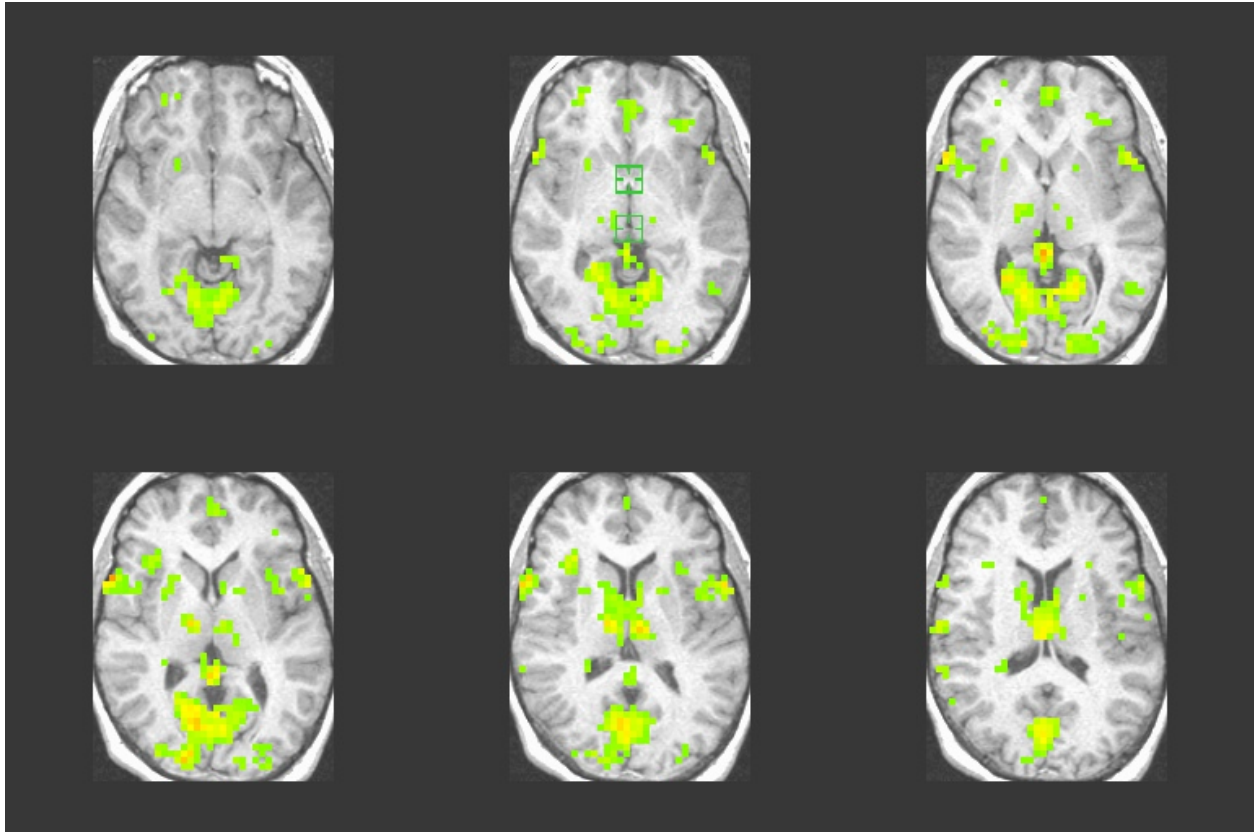


**Figure 17.** In the older adult group, clusters demonstrating a significant main effect of time ( $p < 0.0001$ , cluster threshold = 5) in response to the finger tapping task. Areas of significant putamen activation are seen in both the left and right nuclei.

Surprisingly, no active putamen clusters were found at the  $p < 0.0001$  threshold in the young adult subjects. At an exploratory threshold of  $p < 0.0005$  and a cluster threshold of three voxels, a main effect of time was found in the right putamen. The extent of this activation is shown in Figure 18.

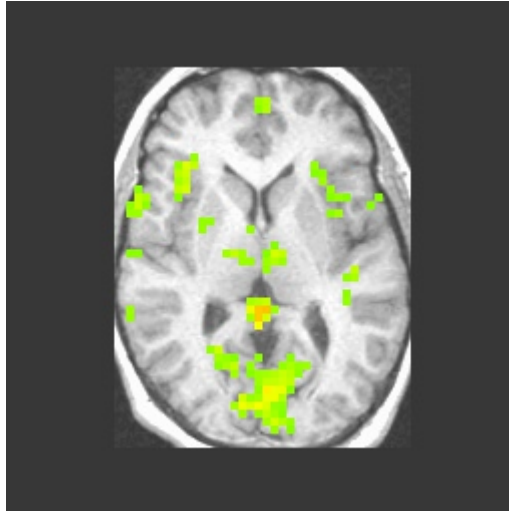


**Figure 18.** In the young adults, a right putamen cluster demonstrating a significant main effect of time in response to the finger tapping task.

While the right putamen cluster found in the young subjects was near to the right cluster found in the old group, it was not overlapping. Instead, the cluster defined for the young group was slightly posterior to that defined for the old. It is interesting to note that although the young group's right putamen activation did not survive the stringent threshold that was surpassed by the older group's activation, the relatively posterior peak of the young adults' right putamen cluster (Talairach coordinates = [27,-5,8]) was more consistent with the region of the putamen that is considered to be involved in simple motor execution (Gerardin et al., 2004).

Although very different statistical thresholds were used to isolate active clusters in the young and old adult groups, the timecourses from the older adult right putamen cluster ( $p < 0.00005$ ) and the young adult right putamen cluster ( $p < 0.0005$ ) are shown in Figure 19 in order to facilitate preliminary qualitative comparisons of the two groups' responses. In both groups, the associated hemodynamic response functions exhibited a gradual rise

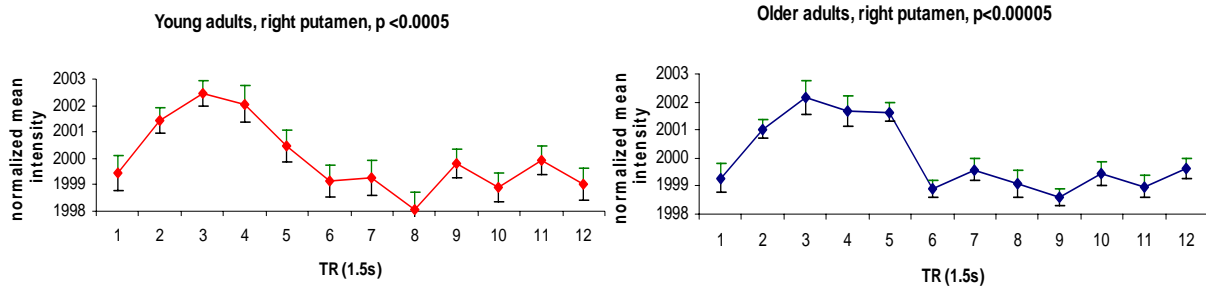


**Figure 19.** Hemodynamic responses extracted from the right putamen for the finger tapping task.

that peaked during the 3-4.5s period following stimulus onset and returned to baseline during the 7.5-9s period following stimulus onset. A qualitative comparison of the timecourses suggests that the two age groups also share a similar peak response amplitude.

### B.2.3 Voxelwise analyses of the two-way group $\times$ time interaction

Voxelwise tests of the two-way group  $\times$  time interaction failed to find any significant effects in the striatum. Outside of the striatal region, a significant effect was found only for a single cluster of three voxels (peak = [-44,-3,14]) that fell between the left insula and Brodmann area 13.

## B.3 DISCUSSION

A better understanding of any age-related effects on striatal activity during a basic visuomotor task would help contribute to our overall understanding of age-related effects in any task in which the striatum is robustly engaged. This preliminary experiment with the finger-tapping task has shown that this paradigm can generate reliable striatal activation in older adults;

furthermore, the resulting hemodynamic response function for the right putamen appears to share a similar shape and peak amplitude as the younger adults' response. However, the present results cannot be interpreted with a great deal of confidence, since (1) the younger adults' response was not significant at our predetermined threshold of  $p < 0.0001$  and (2) the clusters activated in the young and old adults did not share overlapping voxels. Therefore, while these findings support the finger-tapping task as a valid approach for comparing old and young adults' striatal responses to basic motor execution, they also suggest that a greater number of trials or subjects might be required to establish reliable functional effects in both age groups.

## BIBLIOGRAPHY

- Aizenstein, H. J., Clark, K. A., Butters, M. A., Cochran, J., Stenger, V. A., Meltzer, C. C., et al. (2004). The BOLD hemodynamic response in healthy aging. *J Cogn Neurosci*, *16*(5), 786-793.
- Buckner, R. L., Snyder, A. Z., Sanders, A. L., Raichle, M. E., & Morris, J. C. (2000). Functional brain imaging of young, nondemented, and demented older adults. *J Cogn Neurosci*, *12 Suppl 2*, 24-34.
- Cabello, C. R., Thune, J. J., Pakkenberg, H., & Pakkenberg, B. (2002). Ageing of substantia nigra in humans: cell loss may be compensated by hypertrophy. *Neuropathol Appl Neurobiol*, *28*(4), 283-291.
- Cohen, M. S. (1997). Parametric analysis of fMRI data using linear systems methods. *Neuroimage*, *6*(2), 93-103.
- Cools, R., Altamirano, L., & D'Esposito, M. (2006). Reversal learning in Parkinson's disease depends on medication status and outcome valence. *Neuropsychologia*, *44*(10), 1663-1673.
- Cools, R., Lewis, S. J., Clark, L., Barker, R. A., & Robbins, T. W. (2007). L-DOPA disrupts activity in the nucleus accumbens during reversal learning in Parkinson's disease. *Neuropsychopharmacology*, *32*(1), 180-189.
- Cox, R. W. (1996). AFNI: software for analysis and visualization of functional magnetic resonance neuroimages. *Comput Biomed Res*, *29*(3), 162-173.
- Delgado, M. R., Locke, H. M., Stenger, V. A., & Fiez, J. A. (2003). Dorsal striatum responses to reward and punishment: effects of valence and magnitude manipulations. *Cogn Affect Behav Neurosci*, *3*(1), 27-38.
- Delgado, M. R., Nystrom, L. E., Fissell, C., Noll, D. C., & Fiez, J. A. (2000). Tracking the hemodynamic responses to reward and punishment in the striatum. *J Neurophysiol*, *84*(6), 3072-3077.
- Delgado, M. R., Stenger, V. A., & Fiez, J. A. (2004). Motivation-dependent responses in the human caudate nucleus. *Cereb Cortex*, *14*(9), 1022-1030.
- Denburg, N.L., Recknor, E.C., Bechara, A., & Tranel, D. (2006). Psychophysiological anticipation of positive outcomes promotes advantageous decision-making in normal older persons. *Int J Psychophysiol*, *61*(1), 19-25.
- D'Esposito, M., Deouell, L. Y., & Gazzaley, A. (2003). Alterations in the BOLD fMRI signal with ageing and disease: a challenge for neuroimaging. *Nat Rev Neurosci*, *4*(11), 863-872.
- D'Esposito, M., Zarahn, E., Aguirre, G. K., & Rypma, B. (1999). The effect of normal aging on the coupling of neural activity to the bold hemodynamic response. *Neuroimage*, *10*(1), 6-14.

- Folstein, M. F., Robins, L. N., & Helzer, J. E. (1983). The Mini-Mental State Examination. *Arch Gen Psychiatry*, 40(7), 812.
- Forman, S. D., Cohen, J. D., Fitzgerald, M., Eddy, W. F., Mintun, M. A., & Noll, D. C. (1995). Improved assessment of significant activation in functional magnetic resonance imaging (fMRI): use of a cluster-size threshold. *Magn Reson Med*, 33(5), 636-647.
- Frank, M. J., Seeberger, L. C., & O'Reilly R, C. (2004). By carrot or by stick: cognitive reinforcement learning in parkinsonism. *Science*, 306(5703), 1940-1943.
- Friston, K., Ashburner, J., Frith, C., Poline, J., JD, H., & Frackowiak, R. (1995). Spatial registration and normalization of images. *Hum Brain Mapp*, 3(3), 165-189.
- Gerardin, E., Pochon, J. B., Poline, J. B., Tremblay, L., Van de Moortele, P. F., Levy, R., et al. (2004). Distinct striatal regions support movement selection, preparation and execution. *Neuroreport*, 15(15), 2327-2331.
- Graybiel, A. M. (2005). The basal ganglia: learning new tricks and loving it. *Curr Opin Neurobiol*, 15(6), 638-644.
- Hariri, A. R., Brown, S. M., Williamson, D. E., Flory, J. D., de Wit, H., & Manuck, S. B. (2006). Preference for immediate over delayed rewards is associated with magnitude of ventral striatal activity. *J Neurosci*, 26(51), 13213-13217.
- Holmes, C. J., Hoge, R., Collins, L., Woods, R., Toga, A. W., & Evans, A. C. (1998). Enhancement of MR images using registration for signal averaging. *J Comput Assist Tomogr*, 22(2), 324-333.
- Huettel, S. A., Singerman, J. D., & McCarthy, G. (2001). The Effects of Aging upon the Hemodynamic Response Measured by Functional MRI. *NeuroImage*, 13(1), 161-175.
- Knutson, B., Adams, C. M., Fong, G. W., & Hommer, D. (2001). Anticipation of increasing monetary reward selectively recruits nucleus accumbens. *J Neurosci*, 21(16), RC159.
- Knutson, B., & Gibbs, S. E. (2007). Linking nucleus accumbens dopamine and blood oxygenation. *Psychopharmacology (Berl)*, 191(3), 813-822.
- Kunig, G., Leenders, K. L., Martin-Solch, C., Missimer, J., Magyar, S., & Schultz, W. (2000). Reduced reward processing in the brains of Parkinsonian patients. *Neuroreport*, 11(17), 3681-3687.
- Larkin, G., Gibbs, S., Nielson, L., Khanna, K., Carstensen, L. L., & Knutson, B. (2006, April). Neural responsiveness to anticipated gain and loss in younger and older adults. Poster presented at the annual meeting of the Cognitive Neuroscience Society, San Francisco, CA.
- Lehericy, S., van de Moortele, P. F., Lobel, E., Paradis, A. L., Vidailhet, M., Frouin, V., et al. (1998). Somatotopical organization of striatal activation during finger and toe movement: a 3-T functional magnetic resonance imaging study. *Ann Neurol*, 44(3), 398-404.
- Marschner, A., Mell, T., Wartenburger, I., Villringer, A., Reischies, F.M., Heekeren, H.R. (2005). Reward-based decision-making and aging. *Brain Research Bulletin*, 67(5), 382-390.
- Mather, M., & Carstensen, L. L. (2005). Aging and motivated cognition: the positivity effect in attention and memory. *Trends Cogn Sci*, 9(10), 496-502.
- Mell, T., Heekeren, H.R., Marschner, A., Wartenburger, I., Villringer, A., & Reischies, F.M. (2005). Effects of aging on stimulus-reward association learning. *Neuropsychologia*, 43(4), 554-563.

- Nieuwenhuis, S., Heslenfeld, D. J., von Geusau, N. J., Mars, R. B., Holroyd, C. B., & Yeung, N. (2005). Activity in human reward-sensitive brain areas is strongly context dependent. *Neuroimage*, *25*(4), 1302-1309.
- O'Doherty, J., Dayan, P., Schultz, J., Deichmann, R., Friston, K., & Dolan, R. J. (2004). Dissociable roles of ventral and dorsal striatum in instrumental conditioning. *Science*, *304*(5669), 452-454.
- Ravel, S., Legallet, E., & Apicella, P. (2003). Responses of tonically active neurons in the monkey striatum discriminate between motivationally opposing stimuli. *J Neurosci*, *23*(24), 8489-8497.
- Raz, N., Gunning-Dixon, F., Head, D., Rodrigue, K. M., Williamson, A., & Acker, J. D. (2004). Aging, sexual dimorphism, and hemispheric asymmetry of the cerebral cortex: replicability of regional differences in volume. *Neurobiol Aging*, *25*(3), 377-396.
- Raz, N., Torres, I. J., & Acker, J. D. (1995). Age, gender, and hemispheric differences in human striatum: a quantitative review and new data from in vivo MRI morphometry. *Neurobiol Learn Mem*, *63*(2), 133-142.
- Richter, W., & Richter, M. (2003). The shape of the fMRI BOLD response in children and adults changes systematically with age. *Neuroimage*, *20*(2), 1122-1131.
- Roitman, M. F., Wheeler, R. A., & Carelli, R. M. (2005). Nucleus accumbens neurons are innately tuned for rewarding and aversive taste stimuli, encode their predictors, and are linked to motor output. *Neuron*, *45*(4), 587-597.
- Schultz, W., Tremblay, L., & Hollerman, J. R. (2000). Reward processing in primate orbitofrontal cortex and basal ganglia. *Cereb Cortex*, *10*(3), 272-284.
- Seymour, B., O'Doherty, J. P., Dayan, P., Koltzenburg, M., Jones, A. K., Dolan, R. J., et al. (2004). Temporal difference models describe higher-order learning in humans. *Nature*, *429*(6992), 664-667.
- Swainson, R., Rogers, R. D., Sahakian, B. J., Summers, B. A., Polkey, C. E., & Robbins, T. W. (2000). Probabilistic learning and reversal deficits in patients with Parkinson's disease or frontal or temporal lobe lesions: possible adverse effects of dopaminergic medication. *Neuropsychologia*, *38*(5), 596-612.
- Talairach, J., & Tournoux, P. (1998). *Co-planar stereotaxic atlas of the human brain: An approach to medical cerebral imaging*. Stuttgart, NY: Thieme Medical Publishers.
- Tricomi, E., Delgado, M., & Fiez, J. (2004). Modulation of caudate activity by action contingency. *Neuron*, *41*(2), 281-292.
- Tricomi, E., Delgado, M. R., McCandliss, B. D., McClelland, J. L., & Fiez, J. A. (2006). Performance feedback drives caudate activation in a phonological learning task. *J Cogn Neurosci*, *18*(6), 1029-1043.
- Williams, Z. M., & Eskandar, E. N. (2006). Selective enhancement of associative learning by microstimulation of the anterior caudate. *Nat Neurosci*, *9*(4), 562-568.
- Woods, R. P., Cherry, S. R., & Mazziotta, J. C. (1992). Rapid automated algorithm for aligning and reslicing PET images. *J Comput Assist Tomogr*, *16*(4), 620-633.
- Woods, R. P., Grafton, S. T., Watson, J. D., Sicotte, N. L., & Mazziotta, J. C. (1998). Automated image registration: II. Intersubject validation of linear and nonlinear models. *J Comput Assist Tomogr*, *22*(1), 153-165.
- Woods, R. P., Mazziotta, J. C., & Cherry, S. R. (1993). MRI-PET registration with automated algorithm. *J Comput Assist Tomogr*, *17*(4), 536-546.

- Wu, M., Carmichael, O., Lopez-Garcia, P., Carter, C. S., & Aizenstein, H. J. (2006). Quantitative comparison of AIR, SPM, and the fully deformable model for atlas-based segmentation of functional and structural MR images. *Hum Brain Mapp*, 27(9), 747-754.
- Wu, M., Mazurkewicz, L., Nable, M., & Aizenstein, H. J. (2006, October). Improved fMRI co-registration with a fully-deformable model. Poster presented at the annual meeting of the Society for Neuroscience, Atlanta, GA.